COPERNICUS
MARINE ENVIRONMENT MONITORING SERVICE

QUALITY INFORMATION DOCUMENT

Mediterranean Sea Production Centre
MEDSEA_ANALYSIS_FORECAST_BIO_006_014

Issue: 1.3

Contributors: A. Teruzzi, L. Feudale, G. Cossarini, S. Salon, G. Bolzon, P. Lazzari

Approval date by the CMEMS product quality coordination team: dd/mm/yyyy

CHANGE RECORD

When the quality of the products changes, the QuID is updated and a row is added to this table. The third column specifies which sections or sub-sections have been updated. The fourth column should mention the version of the product to which the change applies.

Issue	Date	§	Description of Change	Author	Validated By
1.0	31/08/2017	All	Release of V3.2 version of the Med-biogeochemistry at 1/24° resolution	G.Cossarini, S. Salon, G. Bolzon, A. Teruzzi, P. Lazzari, L. Feudale	
1.1	30/4/2018	All	Release of V4.1 version of the Med-biogeochemistry at 1/24° resolution	G.Cossarini, S. Salon, G. Bolzon, A. Teruzzi, P. Lazzari, L. Feudale	
1.2	27/1/2019	All	Release of version at Q2/2019 of the Med-biogeochemistry at 1/24° resolution with BFM version 5 and open boundary at Dardanelles	A. Teruzzi, G.Cossarini, S. Salon, G. Bolzon, P. Lazzari, L. Feudale	Mercator Ocean
1.3	6/12/2019	All	Release of version Q1/2020 of the Med-biogeochemistry at 1/24° resolution with BGC-Argo float assimilation	A. Teruzzi, G. Cossarini, L. Feudale, G. Bolzon, S. Salon	

TABLE OF CONTENTS

I EXECUTIVE SUMMARY

I.1 Products covered by this document

This document describes the quality of the product MEDSEA_ANALYSIS_FORECAST_BIO_006_014, the nominal product for the analysis and forecast of the biogeochemical state of the Mediterranean Sea. The MED Biogeochemistry product includes 3D daily and monthly fields at 1/24° horizontal resolution (which for the Mediterranean basin is about 4 km) of 10 variables grouped in 5 datasets:

PFTC: chlorophyll and phytoplankton carbon biomass;

NUTR: phosphate and nitrate;

BIOL: oxygen and primary production;

CARB: pH (reported on Total Scale) and dissolved inorganic carbon;

CO2F: surface partial pressure of CO2 and surface CO2 flux.

The CMEMS products can be acknowledged using the following citation:

Bolzon G., Cossarini G., Lazzari P., Salon S., Teruzzi A., Feudale L., Di Biagio V., and Solidoro C. "Mediterranean Sea Biogeochemical Analysis and Forecast (CMEMS MED-Biogeochemistry 2018-Present)." Copernicus Monitoring Environment Marine Service (CMEMS), 2020. https://doi.org/10.25423/CMCC/MEDSEA_ANALYSIS_FORECAST_BIO_006_014_MEDBFM3.

I.2 Summary of the results

The quality of the product MEDSEA_ANALYSIS_FORECAST_BIO_006_014 for Mediterranean Sea biogeochemistry analysis and forecasts has been assessed over the period 1/1/2017-31/12/2017 by means of comparison with independent data (observational in-situ datasets), semi-independent data (satellite and BGC-Argo float datasets) and literature estimates. A detailed and scientific description of the MedBFM model system and of the validation framework is in Salon et al. (2019). The main results of the present quality product assessment are summarized in the following points:

Chlorophyll: it is the mass concentration of chlorophyll a in sea water. In the CMEMS catalogue, the unit of chlorophyll is [mg m^{-3}]. Results give evidence of the model capability of reproducing spatial patterns, seasonal cycle with surface winter bloom period, and the related vertical properties at mesoscale and weekly temporal scale. At surface, the western open sea sub-basins are generally characterized by higher uncertainty and variability (estimated by the RMSD) than eastern ones, with a basin-averaged RMSD of 0.04 (0.01) mg m^{-3} in winter (summer). In the coastal areas the basin-averaged uncertainty rises up to 0.29 (0.33) mg m^{-3} in winter (summer), with higher values in areas more affected by river inputs and shelf dynamics, and a general model underestimation of the high values of observed chlorophyll. The use of the available BGC-Argo floats data showed model consistency in reproducing the key mechanisms coupling physics and biogeochemistry at mesoscale and along the vertical dynamics. The mean RMSD of model and vertical chlorophyll observations from BGC-Argo floats is 0.04 mg m^{-3}. Further, to quantify the model skill to reproduce these key properties we used some novel metrics: averaged content of chlorophyll in the photic layer (0-200m), depth of Deep Chlorophyll Maximum (DCM) and thickness of the winter bloom layer (WLB). Considering areas with a sufficient number of float profiles per month, the modelled averaged content of chlorophyll in the photic layer (0-200m) has a mean RMSD

of 0.04 mg m^{-3}, the DCM is reproduced with an uncertainty of around 12 m, while WLB has an uncertainty of 34 m.

Phytoplankton carbon biomass: it is the carbon mole concentration of phytoplankton in sea water. In the CMEMS catalogue the unit of phytoplankton carbon biomass is [mmol m^{-3}]. No validation metrics are feasible due to the lack of a reliable reference dataset. Consistency of the model formulation (discussed in several scientific papers) and validation of phytoplankton chlorophyll provide an indirect proof of the accuracy for this variable.

Primary production: it is the net primary production of carbon per unit of volume in sea water and it is reported in [mg m^{-3} day^{-1}]. Comparison with literature shows that the simulation consistently reproduces basin-scale and sub-basin-scale patterns and estimates.

Phosphate: it is the mole concentration of phosphate expressed in [mmol m^{-3}]. Uncertainties at basin scale (measured in terms of RMSD) are 0.02 mmol m^{-3} in the upper 60 m and 0.03 mmol m^{-3} in the deeper layers. Basin-scale absolute BIAS along the vertical layers is between 0.01 and 0.02 mmol m^{-3}. General basin-wide gradients and vertical profile shapes are simulated consistently with respect to observations (correlation higher than 0.95, except adr1), with mean monthly vertical profiles within the observed climatological variability.

Nitrate: it is the mole concentration of nitrate expressed in [mmol m^{-3}]. Major horizontal spatial gradients (sub-basin wide patterns) and vertical patterns are consistent with observations (correlation higher than 0.96). Mean monthly vertical profiles are within the observed climatological variability, and uncertainty (i.e. RMSD) at basin scale is 0.40 mmol m^{-3} in the upper 60 m and around 0.70 mmol m^{-3} in the deeper layers. The use of the BGC-Argo floats data corroborates the model consistency in reproducing the key mechanisms coupling physics and biogeochemistry at mesoscale and along the vertical dimension. The mean RMSD of model and vertical nitrate observations from BGC-Argo floats is 0.51 mmol m^{-3}. Further, to quantify the model skill to reproduce key vertical characteristics we use 2 novel metrics: the averaged content of nitrate in the photic layer (0-200m) and the depth of the nitracline. Considering areas with a sufficient number of float profiles per month, the modelled averaged nitrate in the 0-200m layer has a mean RMSD of 0.47 mmol m^{-3}, the nitracline depth is reproduced with a mean uncertainty (RMSD) of 23 m.

Oxygen: it is the mole concentration of dissolved molecular oxygen expressed in [mmol m^{-3}]. Considering the comparison of model results with climatological vertical profile, the basin-scale uncertainties do not exceed 7 mmol m^{-3}. Model profiles are in agreement with climatology (correlation higher than 0.94) and generally within the observed variability. Model outputs consistently reproduce the oxygen weekly dynamics at the mesoscale and its vertical properties, with an overall BIAS between 5 and 35 mmol m^{-3} and a mean RMSD equals to 18 mmol m^{-3}.

Dissolved Inorganic Carbon: in the CMEMS catalogue, dissolved inorganic carbon (DIC) is expressed in [mol m^{-3}], however the present document reports the DIC results in [µmol kg^{-1}] which is the common unit used for in-situ observations. The sea water density is needed for the conversion. Considering the comparison of model results with climatological vertical profile, the basin-scale uncertainties of DIC and Alkalinity (the other master variable of the carbonate system) are 14 and 12 µmol kg^{-1}, respectively.

pH: pH is reported in total scale and at in-situ conditions (i.e., at the temperature, salinity and pressure conditions of the water parcel). Uncertainty of modelled pH is 0.015 according to the comparison with reconstructed climatological vertical profiles among the different Mediterranean sub-basins.

Surface partial pressure of CO2: the CMEMS catalogue provides the 2D surface partial pressure of carbon dioxide expressed in Pascal [Pa]. Validation results report pCO2 in [µatm]: the conversion is 1 µatm equals to 101.325 kPa. Uncertainty of modelled pCO2 is 24 µatm according to the comparison with

climatological vertical profiles among the different Mediterranean sub-basins. Uncertainty of the surface pCO2, estimated using the SOCAT dataset, is about 49 µatm; the comparison shows the good agreement of the model to simulate seasonal cycle and spatial heterogeneity among sub-basins.

Surface flux of CO2: it is the surface downward (i.e., positive values indicate sink of atmospheric CO2 in to the sea) mass flux of carbon dioxide expressed in carbon and reported in [kg m^{-2} s^{-1}] in the CMEMS catalogue. Validation of the air-sea CO2 flux, which uses the unit of [mmol m^{-2} d^{-1}], is based on the comparison with the climatology published in the Chapter 1.7 Air-to-sea carbon flux of the Ocean State Report #2 (Von Schuckmann et al., 2018). Present CO2 flux estimates are consistent with the multi-decadal climatology both in term of seasonal cycle and spatial gradients.

I.3 Estimated Accuracy Numbers

Chlorophyll [mg/m³]				
	RMSD		BIAS	
	win	sum	win	sum
OPEN SEA				
Mod-Sat	0.04	0.01	0.02	0.00
log_{10}(Mod)-log_{10}(Sat)	0.10	0.06	0.06	0.01
COASTAL AREAS				
Mod-Sat	0.29	0.33	-0.05	-0.07
log_{10}(Mod)-log_{10}(Sat)	0.17	0.18	0.01	-0.07

Table I.1. Mean RMSD and BIAS (model minus satellite) of surface chlorophyll [mg m^{-3}] over the open sea and coastal areas of the Mediterranean Sea. Winter corresponds to January to April, summer corresponds to June to September.

	RMSD									
LAYERS (m)	**0-10**	**10-30**	**30-60**	**60-100**	**100-150**	**150-300**	**300-600**	**600-1000**	**Whole column (0-1000)**	**CORR**
PHOSPHATE [mmol/m³]	0.02	0.02	0.02	0.03	0.04	0.03	0.03	0.02	0.03	0.85
NITRATE [mmol/m³]	0.42	0.29	0.45	0.83	0.76	0.68	0.72	0.36	0.56	0.79
OXYGEN [mmol/m³]	4.94	5.04	5.83	6.11	4.73	4.32	6.73	3.51	5.15	0.86

Table I.2. Basin-scale mean RMSD and correlation of phosphate, nitrate and oxygen estimated by comparing the present qualification run and a reference vertical profile climatology based on in-situ observations.

Variables	RMSD
NITRATE [mmol/m³]	0.51
OXYGEN [mmol/m³]	18
Chlorophyll [mg/m³]	0.04

Table I.3. Basin-scale mean RMSD of nitrate and oxygen estimated by comparing the present qualification run and vertical profiles from BGC-Argo floats.

Variables	RMSD
DIC [µmol/kg]	14.0
Alkalinity [µmol/kg]	12.0
pH	0.015
pCO2 [µatm]	24.9

Table I.4. Basin-scale mean RMSD of DIC, Alkalinity, pH (i.e., pH in total scale and in-situ condition) and partial pressure of carbon dioxide in seawater (pCO2) based on the comparison with a reference vertical profile climatology.

Variables	RMSD
Surface pCO2 [µatm]	49

Table I.5. Surface basin-scale mean RMSD of pCO2 based on the comparison with SOCAT dataset.

II PRODUCTION SYSTEM DESCRIPTION

II.1 Production centre details

a) **Production centre name**: Med-MFC

b) **Production subsystem name**: Med-MFC-biogeochemistry

c) **Production Unit**: OGS – Istituto Nazionale di Oceanografia e di Geofisica Sperimentale (Italy)

Description

The biogeochemical analysis and forecasts for the Mediterranean Sea at 1/24 degree are produced by means of the MedBFM model system (i.e. the physical-biogeochemical OGSTM-BFM model coupled with the 3DVARBIO assimilation scheme). MedBFM model is run by OGS and uses as physical forcing the outputs of the NEMO-OceanVar model system (managed by CMCC). Seven days of analysis are produced weekly on Tuesday, with assimilation of surface chlorophyll concentration from satellite observations (provided by the CMEMS-OCTAC) and of vertical profiles of chlorophyll and nitrate from BGC-Argo floats (provided by CORIOLIS and LOV data centres). One day of hindcast and ten days of forecast are produced daily.

The analysis and forecast products are released after completion of the Med-PHY workflow (Fig II.1). On Tuesday, the workflow consists of 7 days of analysis (-8 to -2), one day of hindcast (-1) and 10 days of forecast (0 to 9). From Wednesday to Monday, the workflow consists of one day of hindcast and 10 days of forecast. The data assimilation cycle (Tuesday run) uses the satellite chlorophyll (i.e., a composite average in the range of ±3 days) at 12:00 UTC of the Monday of the previous week (day -8) and the in situ vertical profiles of chlorophyll and nitrate at 12:00 UTC from day -8 to day -2. On day -8, satellite and float assimilation is performed disjointedly.

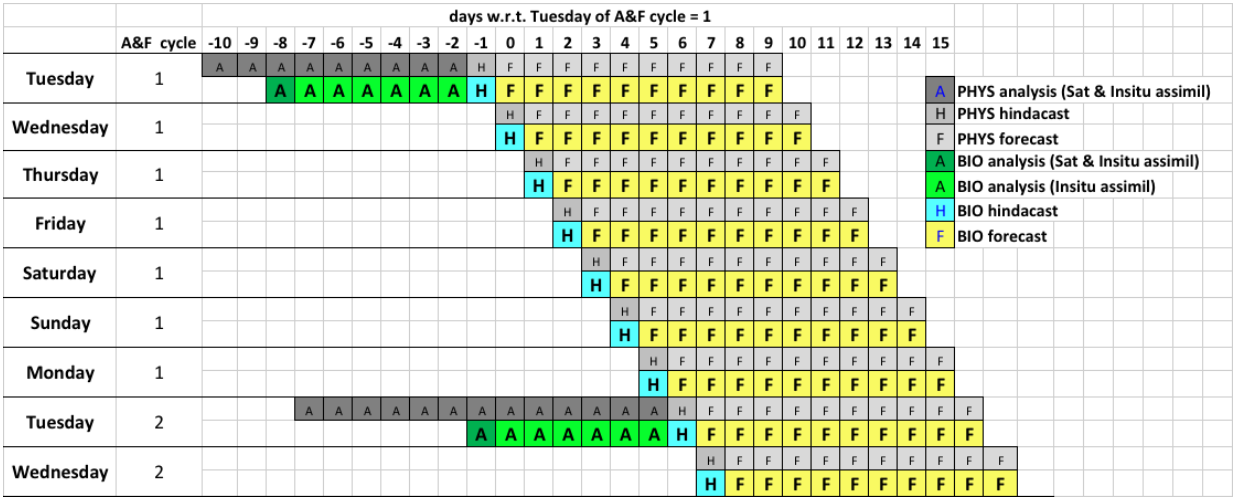

Figure II.1. Scheme of the functioning of the Med-MFC-biogeochemistry system (Med-BIO) for analysis and forecast. Dark, regular and light grey boxes represent the days of analysis, hindcast and forecast of the Med-PHY. Green, blue and yellow boxes represent the days of analysis, hindcast and forecast of the Med-BIO workflow. The production week days when the workflow is executed are reported on the left column.

II.2 Description of the MedBFM v3.1 model system

The Med-biogeochemistry products are provided by the MedBFM v3.1 model system. MedBFM v3.1 consists of the coupled physical-biogeochemical OGSTM-BFM model and the 3DVarBio assimilation scheme (Salon et al., 2019; Lazzari et al., 2010, 2012, 2016; Cossarini et al., 2015; Teruzzi et al., 2014, 2018, 2019; Cossarini et al., 2019). The OGSTM-BFM is designed with a transport model based on the OPA system and a biogeochemical reactor featuring the Biogeochemical Flux Model (BFM), while 3DVarBio is the data assimilation scheme for the correction of phytoplankton functional type and nutrient (i.e., nitrate and phosphate) variables using surface chlorophyll from satellite observations and vertical profiles of chlorophyll and nitrate from BGC-Argo floats (Fig.II.2).

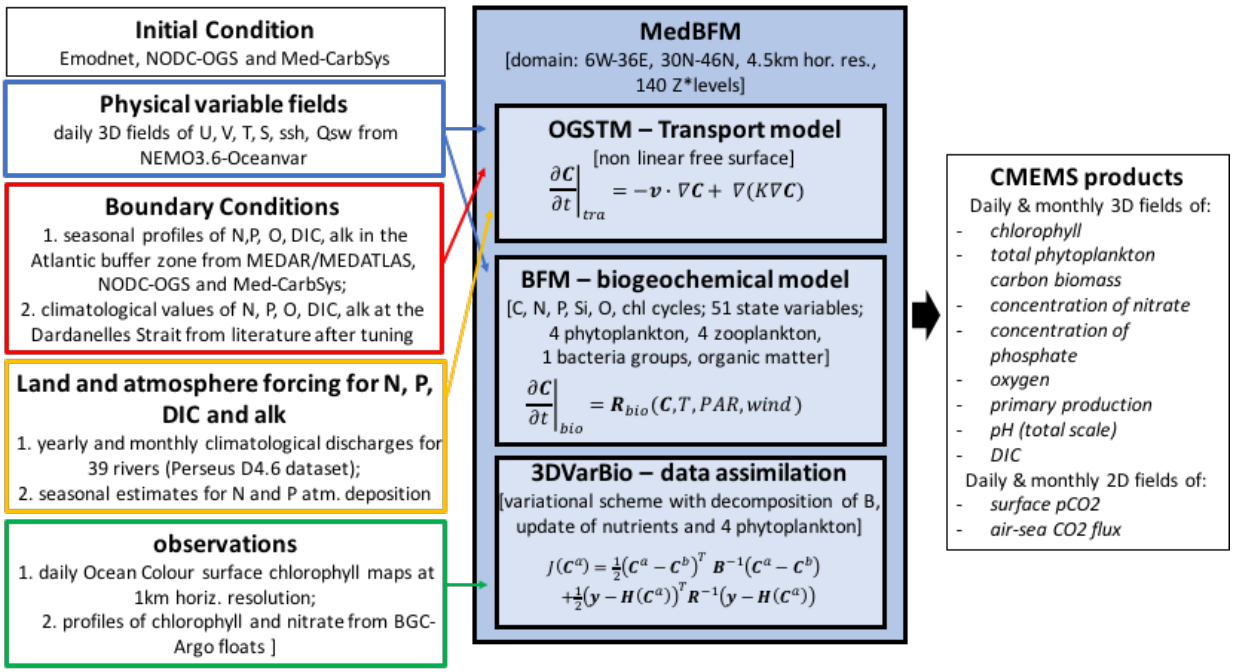

Figure II.2. The Med-BIO model system and interfaces with other components of CMEMS system.

The OGSTM 4.0 transport model is a modified version of the OPA 8.1 transport model (Foujols et al., 2000), which resolves the advection, the vertical diffusion and the sinking terms of the tracers (biogeochemical variables). The OGSTM resolves the free surface and variable volume layer effects on the transport of tracers being fully consistent with NEMO3.6 vvl output provided by Med-PHY. The meshgrid is based on 1/24° longitudinal scale factor and on 1/24°cos(ϕ) latitudinal scale factor. The vertical meshgrid accounts for 141 vertical z-levels (125 active in the Mediterranean domain): 35 in the first 200 m depth, 60 between 200 and 2000 m, 30 below 2000 m. The temporal scheme of OGSTM is an explicit forward time scheme for the advection and horizontal diffusion terms, whereas an implicit time step is adopted for the vertical diffusion.

The sinking term is a vertical flux, which acts on a sub-set of the biogeochemical variables (particulate matter and phytoplankton groups). Sinking velocity is fixed for particulate matter and dependent on nutrients for two phytoplankton groups (diatoms and dinoflagellates).

The daily mean physical dynamics (i.e. the forcing fields) are off-line coupled with the transport-biogeochemical processes, and are pre-computed by the Med-PHY model system, which supplies the temporal evolution of the fields of horizontal and vertical current velocities, vertical eddy diffusivity,

potential temperature, salinity, sea surface height in addition to surface data for solar shortwave irradiance and wind stress (see section on upstream data and boundary conditions for further details).

The features of the biogeochemical reactor BFM (Biogeochemical Flux Model) have been chosen to target the energy and material fluxes through both “classical food chain” and “microbial food web” pathways (Thingstad and Rassoulzadegan, 1995), and to take into account co-occurring effects of multi-nutrient interactions. Both of these factors are very important in the Mediterranean Sea, wherein microbial activity fuels the trophodynamics of a large part of the system for much of the year and both phosphorus and nitrogen can play limiting roles (Krom et al., 1991; Bethoux et al., 1998).

BFMv5 model (i.e., the official version released by www.bfm-community.eu) describes the biogeochemical cycles of 4 chemical compounds: carbon, nitrogen, phosphorus and silicon through the dissolved inorganic, living organic and non-living organic compartments (Figure II.3). The model includes nine plankton functional types (PFTs). Phytoplankton PFTs are diatoms, flagellates, picophytoplankton and dinoflagellates. Heterotrophic PFTs consists of carnivorous and omnivorous mesozooplankton, bacteria, heterotrophic nanoflagellates and microzooplankton. Nitrate and ammonia are considered for the dissolved inorganic nitrogen. The non-living compartment consists of 3 groups: labile, semilabile and refractory organic matter. The first two are described in terms of carbon, nitrogen, phosphorus and silicon contents. The model is fully described in Lazzari et al. (2012, 2016), where it was corroborated for chlorophyll, primary production and nutrients in the Mediterranean Sea for a 1998-2004 simulation. The BFM model is also coupled to a carbonate system model (Cossarini et al., 2015, Melaku Canu et al., 2015), which consists of three prognostic state variables: alkalinity (ALK) and dissolved inorganic carbon (DIC) and particulate inorganic carbon (PIC) which are driven by biological processes (i.e. photosynthesis, respiration, precipitation and dissolution of CaCO3, nitrification, denitrification, and uptake and release of nitrate, ammonia and phosphate by plankton cells) and physical processes (exchanges at air-sea interface and dilution-concentration due to evaporation minus precipitation process). In particular, PIC precipitation occurs in correspondence of phytoplankton mortality and grazing by zooplankton (Orr et al., 2017). Dissolution of PIC occurs for oversaturated calcite conditions according to Berner and Morse (1972). pCO2 and pH (expressed in total scale) are calculated at the in-situ temperature and pressure conditions using Mehrbach et al. (1973) refit by Lueker et al. (2000). Formulations for the kinetic constants of thermodynamic equilibrium of carbon acid dissociation as prescribed in Orr and Epitaloni (2015). CO2 air-sea gas exchange formulation is computed according to updates provided by Wanninkhof (2014).

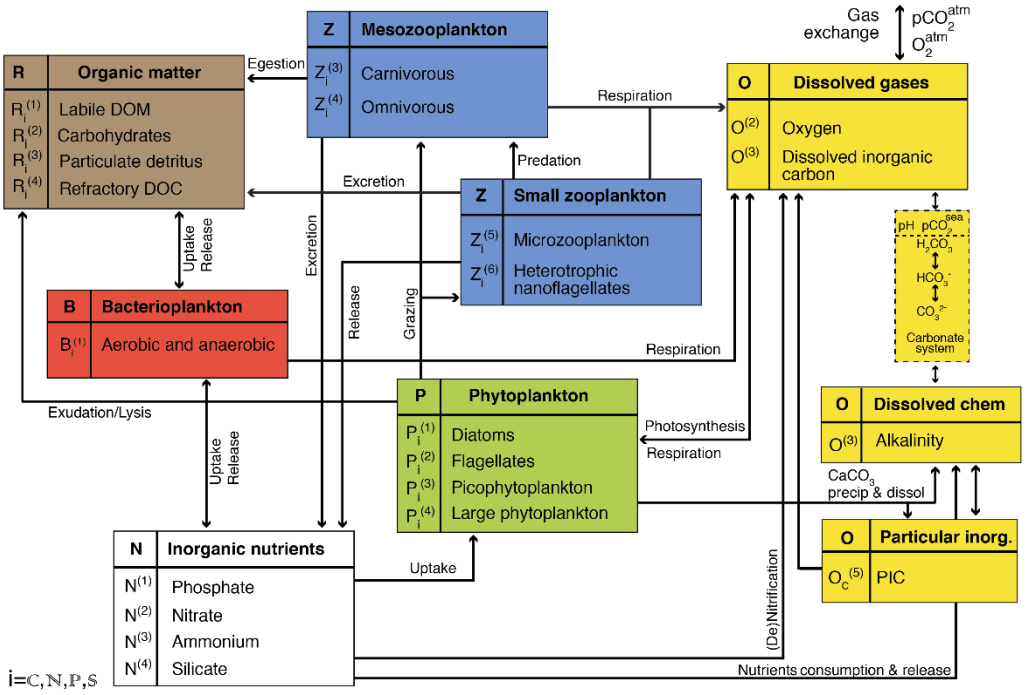

Figure II.3. Scheme of the state variables and significant processes of the upgraded Biogeochemical Flux Model (BFM) version 5.

II.3 Description of the Data Assimilation scheme

1. The data assimilation of the surface chlorophyll concentration and of the vertical insitu profiles of chlorophyll and nitrate is performed through a variational scheme (3DVarBio) during the 7 days of analysis of the Tuesday run of Fig. II.1 (see details on 3DVarBio in Teruzzi et al., 2014, 2018, 2019 and Cossarini et al., 2019). The surface chlorophyll concentration is provided by satellite observations produced by the OCTAC; the insitu vertical profiles of chlorophyll and nitrate are provided by BGC-Argo floats data made available by CORIOLIS and LOV.
2. The data assimilation corrects the four phytoplankton functional groups (17 state variables including carbon, chlorophyll, nitrogen phosphorus and silicon internal quotas) and two nutrients (i.e., phosphate and nitrate) of the BFM. The 3DVarBio scheme decomposes the background error covariance matrix using a sequence of different operators that account separately for the vertical covariance (Vv), the horizontal covariance (Vh) and the covariance among biogeochemical variables (Vb). Vv is defined by a set of synthetic profiles that are evaluated by means of an Empirical Orthogonal Function (EOF) decomposition applied to a validated multi-annual 1998-2015 run (Teruzzi et al., 2018). EOFs are computed for 12 months and 30 coastal and open sea sub-regions in order to account for the variability of 3D chlorophyll and nitrate anomaly fields. The assimilation is performed from 0 to 600 meters for chlorophyll and nitrate profiles, and from 0 to 200 meters for satellite chlorophyll. Vh is built using a Gaussian filter whose correlation radius modulates the smoothing intensity. A non-uniform and direction-dependent correlation radius has been implemented (Teruzzi et al., 2018, Cossarini et al., 2019). Vb operator consists of monthly and sub-region varying covariances among the biogeochemical variables. Further, Vb operator maintains the ratio among the phytoplankton groups and preserves the physiological status of the phytoplankton cells (i.e. preserve optimal values for the internal chlorophyll and carbon nutrients quota).

3. The operational workflow of the analysis run (the Tuesday row in Fig. II.1) consists of a sequence of seven days of assimilation: the satellite surface chlorophyll map (i.e., a composite average in the range of ±3 days) is assimilated at 12:00 UTC of the previous Monday (i.e., day -8) and the insitu vertical profiles of chlorophyll and nitrate are assimilated at 12:00 UTC from day -8 to day -2. A pre-processing quality control is applied prior of the assimilation:
    - Ocean Color chlorophyll daily data (±3 days maps of L3 CMEMS product) are checked for spikes (i.e., values whose anomalies is higher than 3 times the daily climatology standard deviation), temporally averaged (i.e., geometric means) and spatially interpolated (i.e., linear operator) on the model grid. Surface chlorophyll values with misfit higher than 10 mg/m^3 are rejected.
    - BGC-Argo float chlorophyll profiles (daily data from Coriolis data repository) are checked for negative values (rejection); the quenching correction (based on Xing et al., 2012) is performed by imposing a constant Chl value in the MLD (as done in LOV PQ repository; Schmechtig et al., 2018). Additionally during assimilation, if the misfit model minus observation is higher than 5 mg/m^3 the profile is rejected.
    - BGC-Argo float nitrate profiles (daily data from Coriolis and LOV data repository) are fine tuned for the Mediterranean Sea (Mignot et al., 2019) and profiles are rejected if surface value is higher than 3 mmol/m^3. Additionally during assimilation, a profile is rejected if the misfit at surface is higher than 1 mmol/m^3 (i.e., condition requested for at least 5 points in the 0-50 m layer); observations in the layer 250-600m are rejected if their misfits are higher than 2.5 mmol/m^3.

II.4 Upstream data and boundary conditions

The CMEMS–Med-MFC-Biogeochemistry system uses the following upstream data:

1. Initial conditions of biogeochemical variables are set as sub-basin (Fig. III.1) climatological profiles computed from the in-situ EMODnet data collections (EMODnet, 2018) integrated with additional dataset listed in Lazzari et al. (2016) and Cossarini et al. (2015). A spin-up period (4 months) is carried out to reach the start date of the simulation (1/1/2017).
2. The physical ocean (current, temperature, salinity, vertical eddy viscosity, SSH) and atmospheric (short wave radiation and wind stress) forcing daily fields are obtained from MEDSEA_ANALYSIS_FORECAST_PHY_006_013 produced by Med-PHY.
3. The surface chlorophyll is obtained from the satellite multi-sensor (MODIS and VIIRS) product OCEANCOLOUR_MED_CHL_L3_NRT_OBSERVATIONS_009_040.
4. The insitu vertical profiles of chlorophyll (Schmechtig et al., 2015) and nitrate (Johnson et al., 2018) are obtained from Coriolis Data Assembly Center (as described in Bittig et al., 2019) after PQ procedures implemented at LOV data repository (as described in Schmechtig et al., 2018).
5. The biogeochemical boundary conditions in the Atlantic buffer zone (i.e. the area to the western of the Gibraltar Strait in Fig. III.1) are provided through a Newtonian dumping term. The tracer concentrations are relaxed to climatological seasonally varying profiles. Seasonal profiles of phosphate, nitrate, silicate, dissolved oxygen are derived from an analysis of the climatological MEDAR-MEDATLAS and NODC-OGS datasets, while climatological annual profiles of ALK and DIC are obtained from in-situ datasets (Huertas et al., 2009; de la Paz et al., 2011; Alvarez et al., 2014).
6. The biogeochemical open boundary conditions at the Dardanelles Strait are provided through a Dirichlet-type scheme. The values of nitrate, phosphate, silicate, DIC, alkalinity at the open boundary are set to constant values using literature information (Yalcin et al., 2017; Tugrul et

al., 2002; Souvermezoglou et al., 2014; Copin, 1993; Schneider et al., 2007) after a tuning based on the consistency of modelled fluxes with published flux estimates (Perseus D4.6; Yalcin et al., 2017; Tugrul et al. 2002; Copin, 1993) and modelled tracer concentrations in the northern Aegean Sea with published observations (Souvermezoglou et al., 2014; Krasakopoulou et al., 2017). A radiative condition at the open boundary is set for the other BFM tracers.

7. Atmospheric deposition rates of inorganic nitrogen and phosphorus were set according to the synthesis proposed by Ribera d'Alcalà et al. (2003) and based on measurements of field data (Loye-Pilot et al., 1990; Guerzoni et al., 1999; Herut and Krom, 1996; Cornell et al., 1995; Bergametti et al., 1992). Atmospheric deposition rates of nitrate and phosphate were assumed to be constant in time during the simulation year, but with different values for the western (580 Kt N yr^{-1} and 16 Kt P yr^{-1}) and eastern (558 Kt N yr^{-1} and 21 Kt P yr^{-1}) sub-basins. The rates were calculated by averaging the "low" and "high" estimates reported by Ribera d'Alcalà et al. (2003).
8. Terrestrial inputs of nutrient (N and P) from 39 rivers, which are aligned with the Med-PHY configuration, are obtained from the PERSEUS FP7-287600 project dataset (deliverable D4.6). The nutrient discharge rates are climatological (average of the 2000-2015 period) and take into account seasonal variability on a monthly scale based on monthly varying water discharge. The 39 rivers, as shown in Fig. III.1, are Nile, Vjosë, Seman, Buna/Bojana, Piave, Tagliamento, Soca/Isonzo, Livenza, Brenta-Bacchiglione, Adige, Lika, Reno, Krka, Arno, Nerveta, Aude, Trebisjnica, Tevere/Tiber, Mati, Volturno, Shkumbini, Struma/Strymonas, Meric/Evros/Maritsa, Axios/Vadar, Arachtos, Pinios, Acheloos, Gediz, Buyuk Menderes, Kopru, Manavgat, Seyhan, Ceyhan, Gosku, Medjerda, Asi/Orontes.
9. Terrestrial inputs of ALK and DIC from 39 rivers are derived considering their typical concentrations per fresh water mass in macro coastal areas of the Mediterranean Sea (Copin, 1993; Meybeck and Ragu, 1995; Kempe et al., 1991) and the river water discharges from the PERSEUS dataset (Deliverable D4.6).
10. Atmospheric pCO2 concentration is set equal to the yearly average measured at the Lampedusa station (Artuso et al., 2009) between 1992 and 2018 (http://cdiac.ess-dive.lbl.gov/ftp/trends/co2/lampedus.co2) with the present-day values extrapolated by linear regression.
11. Surface evaporation-precipitation effects on dilution and concentration of tracers at surface are directly computed by OGSTM through the non-linear free-surface z*-coordinate configuration and using directly the sea surface anomaly evolution provided by the NEMO3.6 output.

1. VALIDATION FRAMEWORK

The CMEMS Med-MFC analysis and forecast system is validated through a qualification run spanning from 1-Jan-2017 to 31-Dec-2017. The products assessed are chlorophyll, net primary production, phosphate, nitrate, oxygen, pH, pCO2, DIC, Alkalinity and CO2 air-sea flux. Currently, Alkalinity is not provided in the Med-MFC analysis and forecast system, but we think it is important to inform the users about the accuracy of this prognostic variable of the carbonate system simulated by BFM model. A quantitative estimate of the phytoplankton biomass uncertainty cannot be provided since the lack of a reference dataset, thus, this product can be validated only in term of model formulation consistency.

Model chlorophyll data are compared with multi-sensor satellite chlorophyll from CMEMS OCTAC OCEANCOLOUR_MED_CHL_L3_NRT_OBSERVATIONS_009_040 using metrics that refer to the "misfits" computed as the differences between satellite chlorophyll (7-days composite map) and the model output before the data assimilation execution (every 7 days). Thus, the metrics (BIAS and Root Mean Square of the differences between model output and satellite observations, RMSD) estimate the skill performance of the forecast (i.e. uncertainty after seven days of free simulation) and are reported as time series for the sub-basins of Fig. III.1. Chlorophyll model outputs are also compared with in-situ observations of chlorophyll concentration from the BGC-Argo floats dataset (Fig. III.4) before the data assimilation execution. BIAS, RMSD, correlation along with novel metrics (e.g., deep chlorophyll maximum depth, integral values and thickness of the layer of the winter bloom) between BGC-Argo profiles and the matching model output profiles (i.e. the model output at the time and location of the in-situ profile) are reported as time series for selected layers (Table III.1) and sub-basins (Fig. III.1) and as average statistics computed from all the matching pairs of model and observation profiles for each sub-basin.

Model net primary production data are compared with literature data based on multi-annual simulation (Lazzari et al., 2012), satellite model (Bosc et al., 2004; Colella, 2006), in-situ estimates (Siokou-Frangou et al., 2010).

Model phosphate, nitrate and dissolved oxygen data are compared with a climatology derived by the EMODnet (2018) and NODC-OGS datasets based on the sub-basins of Fig. III.1. The validation of model variables considers consistency both with the vertical profiles for each sub-basin and with reference values at the layers listed in Table III.1. The EMODnet (2018) integrated with the NODC-OGS dataset (list of datasets in Tab. III.2) spans the period 1997-2016, consists of 15293 (nitrate), 20161 (phosphate) and 151187 (dissolved oxygen) observations, and covers the Mediterranean Sea as shown in Fig. III.3. An additional qualitative comparison is performed using the World Ocean Atlas (WOA2013) climatological dataset.

Nitrate and dissolved oxygen model outputs are also compared with BGC-Argo float data (Fig. III.4) to compute the BIAS, RMSD, correlation and novel metrics (integrated vertical values and depth of nutricline) between BGC-Argo profiles and the model output profiles before the data assimilation execution. The metrics are reported as time series for selected layers (Table III.1) and sub-basins (Fig. III.1) and as average statistics computed from all the matching pairs of model and observation profiles for each sub-basin.

Model DIC, Alkalinity, pH in total scale and pCO2 are compared with a climatology derived by the reference datasets illustrated in Tab. III.3, and Fig. III.3 (CarbSys datasets). The reference dataset considers the period from 1997 to 2015 and includes scientific cruises covering the whole Mediterranean Sea, several scientific cruises in marginal seas and local areas, and a single fixed station (DYFAMED) continuously monitored for several years. Usually, the scientific cruises were conducted during one month, mostly in spring or autumn. The dataset does not resolve the annual cycle and

reasonably estimates the basin wide gradients. The most observed variables are DIC and alkalinity (about 5300 observations), while pH was collected only in less than 30% of the samplings. Thus, pH and pCO2 have been reconstructed using CO2sys software (Lewis and Wallace, 1998) with available DIC, ALK and other regulatory information (i.e., temperature, salinity and concentration of phosphate and silicate). The product quality metric is the RMSD between vertical profiles of a reconstructed climatology and the model outputs on the sub-basins of Fig. III.1.

Moreover, pCO2 has been validated considering the SOCAT v6 Data Collection (Bakker et al., 2016). The dataset consists of surface ocean fugacity (fCO2) measurements (up to 150000 observations) in the Mediterranean Sea covering the period 1998-2016 (Fig. III.5). Fugacity measurements are converted to partial pressure measurements using standard formula. The spatial distribution does not cover uniformly the Mediterranean sub-basins and temporal coverage stops in 2016. Therefore, the comparison is organized by calculating a monthly climatology for the Mediterranean sub-basins (i.e., only 10 out of 16 sub-basins have reliable data), and after an actualization to the temperature effect on solubility for year 2017 was applied. The product quality metric is the RMSD between the model and climatology.

CO2 air-sea flux has been validated by evaluating the consistency of the model results with the MEDSEA_REANALYSIS_BIO_006_008 reanalysis estimates of CO2 air-sea flux published in the Ocean State Report (von Schuckmann et al., 2018).

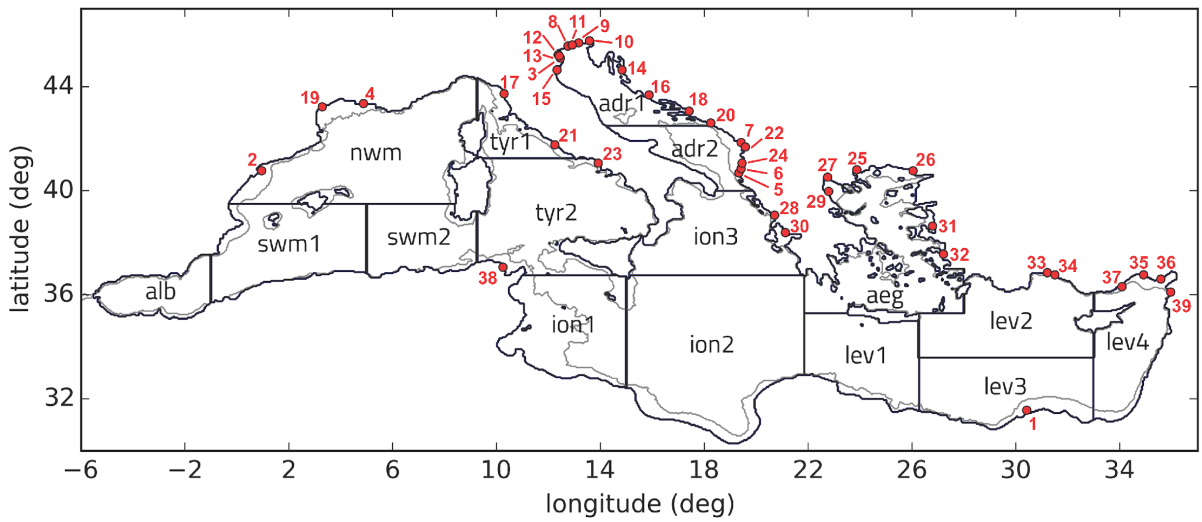

Figure III.1. Subdivision of the model domain in sub-basins used for the validation of the qualification run. According to data availability and to ensure consistency and robustness of the metrics, different subsets of the sub-basins or some combinations among them can be used for the different metrics: lev = lev1+lev2+lev3+lev4; ion = ion1+ion2+ion3; tyr = tyr1+tyr2; adr = adr1+adr2; swm = swm1+swm2. The grey line defines the bathymetric contour at 200 m. Red dots with numbers correspond to main river mouth positions: Nile (1), Ebro (2), Po (3), Rhone (4), Vjosë (5), Seman (6), Buna/Bojana (7), Piave (8), Tagliamento (9), Soca/Isonzo (10), Livenza (11), Brenta-Bacchiglione (12), Adige (13), Lika (14), Reno (15), Krka (16), Arno (17), Nerveta (18), Aude (19), Trebisjnica (20), Tevere (21), Mati (22), Volturno (23), Shkumbini (24), Struma/Strymonas (25), Meric/Evros/Maritsa (26), Axios/Vadar (27), Arachtos (28), Pinios (29), Acheloos (30), Gediz (31), Buyuk Menderes (32), Kopru (33), Manavgat (34), Seyhan (35), Ceyhan (36), Gosku (37), Medjerda (38), Asi/Orontes (39).

Layer 1	Layer 2	Layer 3	Layer 4	Layer 5	Layer 6	Layer 7	Layer 8
0-10	10-30	30-60	60-100	100-150	150-300	300-600	600-1000

Table III.1. Vertical layers (in m) considered for the validation of the qualification run products.

Nutrients and Dissolved oxygen (from EU/MEDAR/MEDATLAS II and OGS-NODC)		
Dataset name	**Period**	**Area**
SINAPSI 3,4	2002-2003	Eastern Med.
JGOFS-FRANCE	1999	Western Med.
BIOPT 6	2006	Eastern Med.
DYFAMED	1998-2007	North-Western Med.
RHOFI 3,2,1	2001-2003	Ligurian Sea
NORBAL 1, 2, 3, 4	2000-2003	Algerian Sea
CIESM SP1,SP2,SP3	1998-2006	Mediterranean
MELISSA	2004, 2007	Western Med.
MEDGOOS 2, 3, 4, 5	2001-2002	Mediterranean
METEOR 51	2001	Western Med.
REGINA MARIS, GARCIA DEL CID	Apr, Sep 2008	Alboran Sea
SESAME ADRIATIC SEA	Apr, Sep 2008	Adriatic Sea
CARBOGIB 01,02,03,04,05,06	2005-2006	Alboran Sea, Gibraltar Strait
METEOR 84/3	2011	Mediterranean

Table III.2. List of datasets gathered through the OGS-NODC that are used to integrate the EMODnet (2018) dataset.

Name	Variables	Period	Location	# data	Reference
METEOR51	DIC, ALK, anc. vars	Oct-Nov 2001	TransMed	253	Schneider et al., 2007
BUOM2008	DIC, ALK, anc. vars	June-July 2008	TransMed	567	Touratier et al., 2011
PROSOPE	DIC, pH@25, anc. vars	Sep-Oct 1999	West Med	188	Begovic and Copin, 2013
METEOR 84/3	DIC, ALK, pH@25, anc. vars	Apr 2011	TransMed	845	Tanhua, et al., 2012.
SESAME-EGEO	DIC, ALK, T,S	Apr and Sep 2008	Aegean Sea	265	http://isramar.ocean.org.il/PERSEUS_Data/
SESAME regina_maris	ALK, pH@25, anc. vars	Apr 2008	Alboran Sea	254	http://isramar.ocean.org.il/PERSEUS_Data/
SESAME Garcia del Cid	ALK, pH@25, anc. vars	Sep 2008	Alboran Sea	331	http://isramar.ocean.org.il/PERSEUS_Data/
SESAME Adriatic	ALK, pH@25, anc. vars	Apr and Sep 2008	Adriatic Sea	333	http://isramar.ocean.org.il/PERSEUS_Data/
CARBOGIB	ALK, DIC, pH@25, anc. vars	May, Sept, Dec 2005; Mar, May, Dec 2006	Alboran Sea	229	Huertas, 2007a
GIFT	ALK, DIC, pH@25, anc. vars	Jun, Nov 2005	Alboran Sea	30	Huertas, 2007b
DYFAMED Station	ALK, DIC	Almost monthly from 1999 to 2004	North West Med	707	Copin-Montegut and Begovic, 2002
MEDSEA 2013	DIC, ALK, T,S	May 2013	TransMed	462	Goyet et al., 2015
MOOSE dyfamed MOOSE-GE 2013-2016	DIC, ALK, T,S	2013-2016	North West Med	700	EMODnet, 2018

Table III.3. List of datasets used to build climatology of the carbonate system variables (CarbSys). "TransMed" refers to the scientific cruise that covered the Mediterranean Sea from the Western sub-basin to the Eastern sub-basin; "anc. vars" refers to ancillary variables (T, S); "pH@25" refers to pH reported at 25°C.

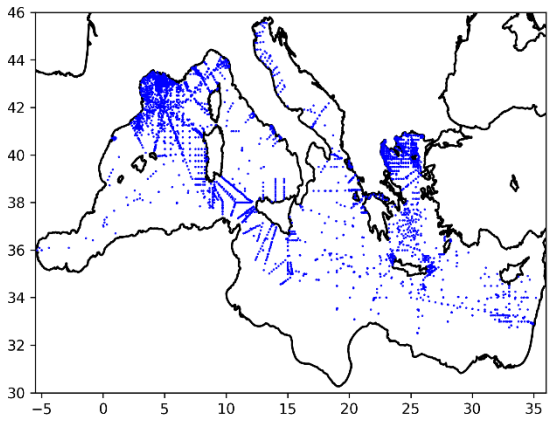

Figure III.2. Map of gathered data of nutrients through the EMODnet (2018) and NODC-OGS datasets for period 1997-2016.

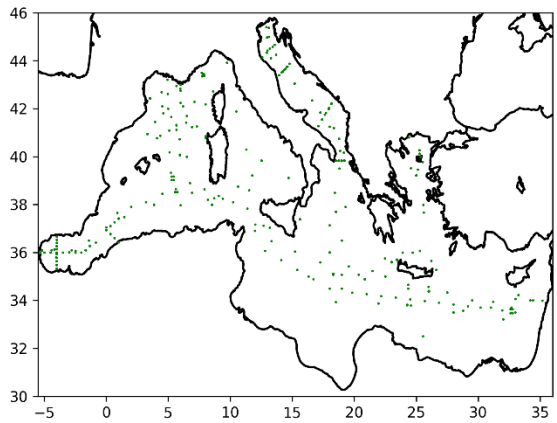

Figure III.3. Location of the carbonate system (CarbSys) datasets for the period 1999-2016 listed in Table III.3.

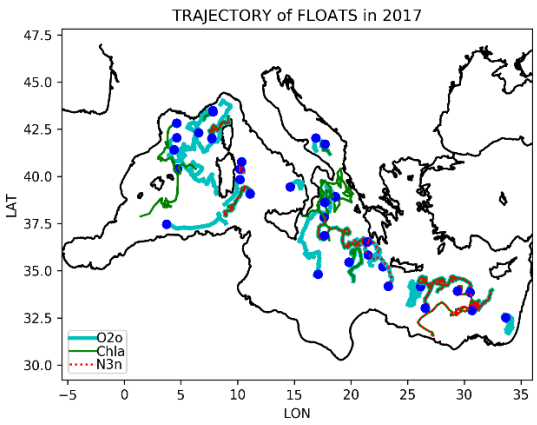

Figure III.4. Trajectories of 30 BGC-Argo floats in 2017 (i.e., 24 oxygen, 17 chlorophyll and 10 nitrate sensors). Data quality described in Bittig et al. (2019).

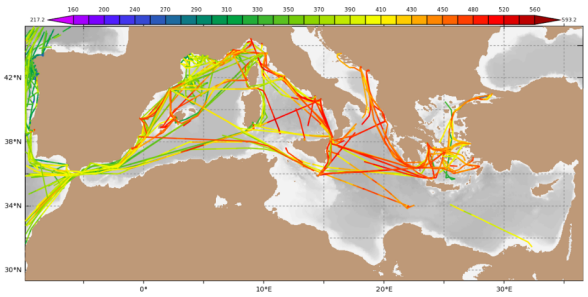

Figure III.5. Map of surface fCO2 observations from the SOCAT dataset for the period 1998-2016.

III VALIDATION RESULTS

III.1 Chlorophyll

Modelled chlorophyll is compared with satellite data in Fig. IV.1 (averaged annual maps of surface chlorophyll) and Fig. IV.2 (time series of weekly mean surface chlorophyll concentration for selected sub-basins). Time series of BIAS and RMS of the differences are plotted in Fig. IV.3 for selected sub-basins. Their seasonal averages, which are computed for both logarithm and natural values, are reported in Tab. IV.1 and IV.2 for open sea and coastal areas, respectively. The coastal areas limit is defined by the model grid isobath at 200m. As well known, Mediterranean Sea is quite heterogeneous, with sub-basins characterized by different biogeochemical dynamics. The general features, widely described in literature and clearly visible in the maps of Fig. IV.1 and in the time series of Fig. IV.2, are the higher concentrations and larger seasonal cycles that characterize the western sub-basins with respect to the eastern ones. The results of the qualification run are thus consistent with satellite observations (Tab. 4.1 and 4.2).

In the open sea areas, western sub-basins have higher uncertainty (i.e. higher RMSD, Fig. IV.3) than eastern sub-basins, however never exceeding 0.10 mg/m^3 (Tab. IV.1). The highest value of RMSD is in the ALB where not well resolved boundary conditions might have impacted phytoplankton dynamics. In general, uncertainties are slightly higher during winter (Fig. IV.3 and Table IV.1) because the variability of the chlorophyll is also higher than during the summer period. The value of the RMSD over the Mediterranean Sea, considering the 2017 average, is 0.04 and 0.001 mg/m^3 for winter and summer, respectively, while BIAS is 0.02 mg/m^3 in winter and 0.01 mg/m^3 in summer (see Tab. IV.1).

Since CMEMS version at Q2/2018, the MedBFM system assimilates chlorophyll data on both coastal and open-sea areas. Thus, MedBFM provides a good model performance also in the coastal areas (see Tab. IV.2). In these areas the model underestimates the satellite product of about 0.05 mg/m^3 and 0.07 in winter and summer, respectively, and the mean RMSD is about 0.29 mg/m^3 and 0.33 mg/m^3, with higher values (between 0.4 and 0.6 mg/m^3) in the Adriatic sub-basins and in the areas close to the Gabes Gulf (ION1, summer) and the Nile river mouth (LEV3). In particular, the peak of RMSD in LEV3 is due to an underestimation of the very local fertilization effect of the Nile input that might be indicating an underestimation of the nutrient input from the PERSEUS project dataset.

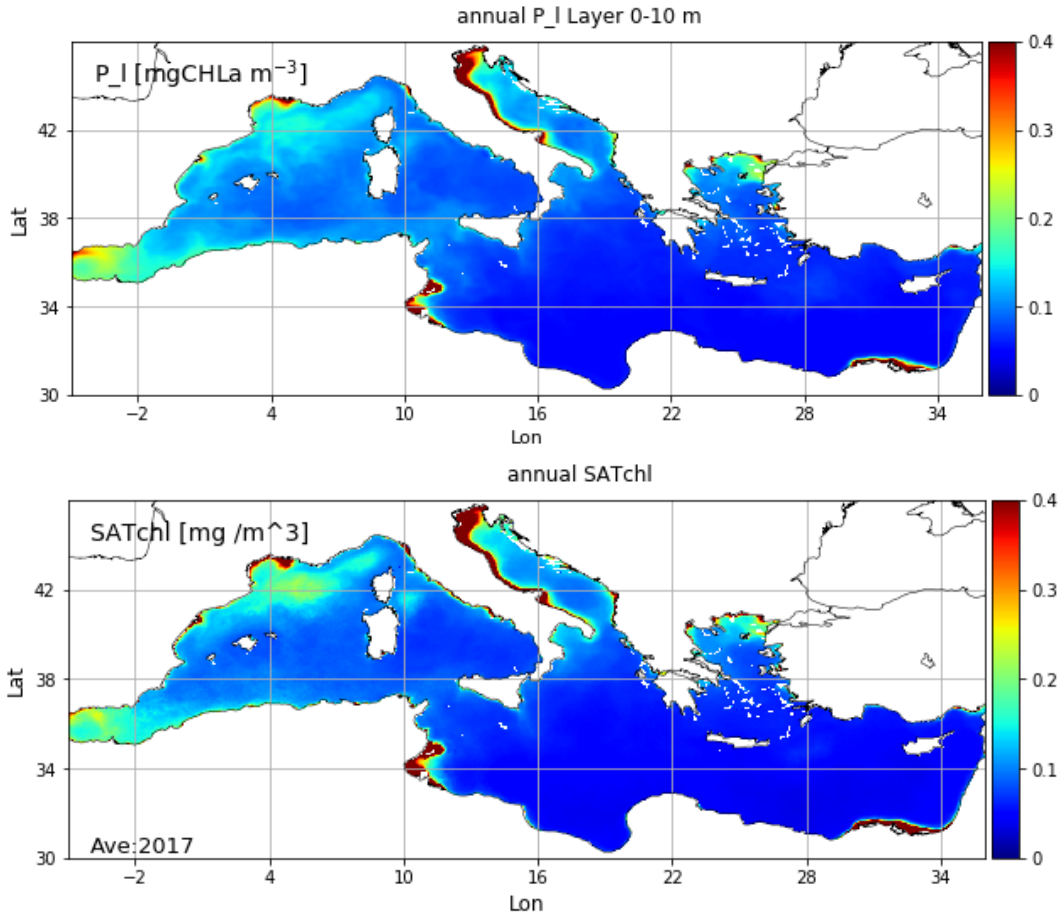

Figure IV.1. 2017 averaged annual maps of surface chlorophyll from qualification run (top) and from NRT multi-sensor satellite (bottom). The average is computed considering the year 2017, and the layer 0-10 m for the model results.

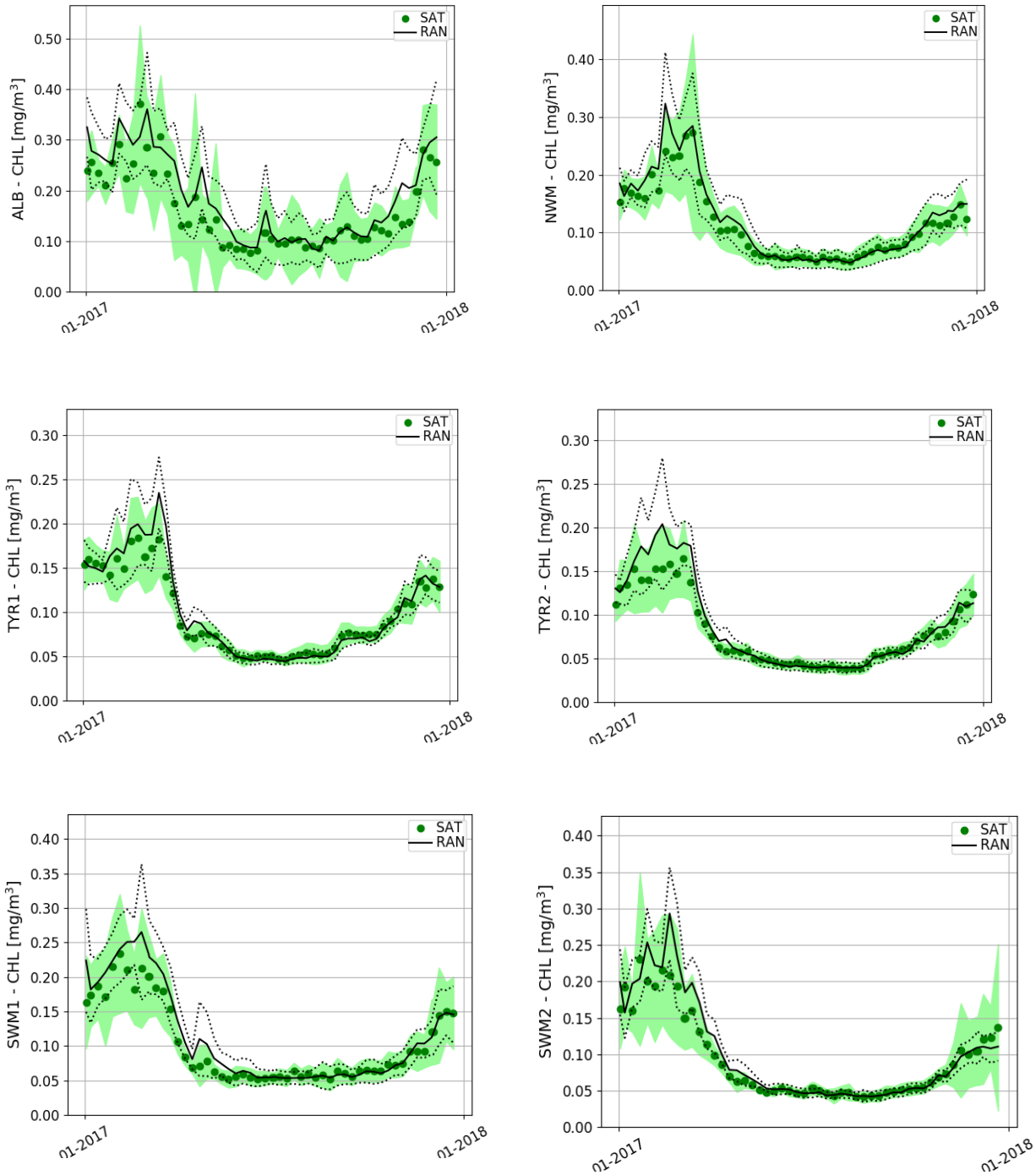

Figure IV.2. Time series of the weekly qualification run mean surface chlorophyll concentration of open sea (black solid line, RAN) with the spatial standard deviation (STD, dotted black line) and the NRT multi-sensor satellite data (green dots, SAT) with its STD (shaded green area) for 12 of the 16 sub-basins of Fig. III.1. Model data (sub-surface 0-10m layer) and satellite data are reported only for open sea areas (continues overleaf).

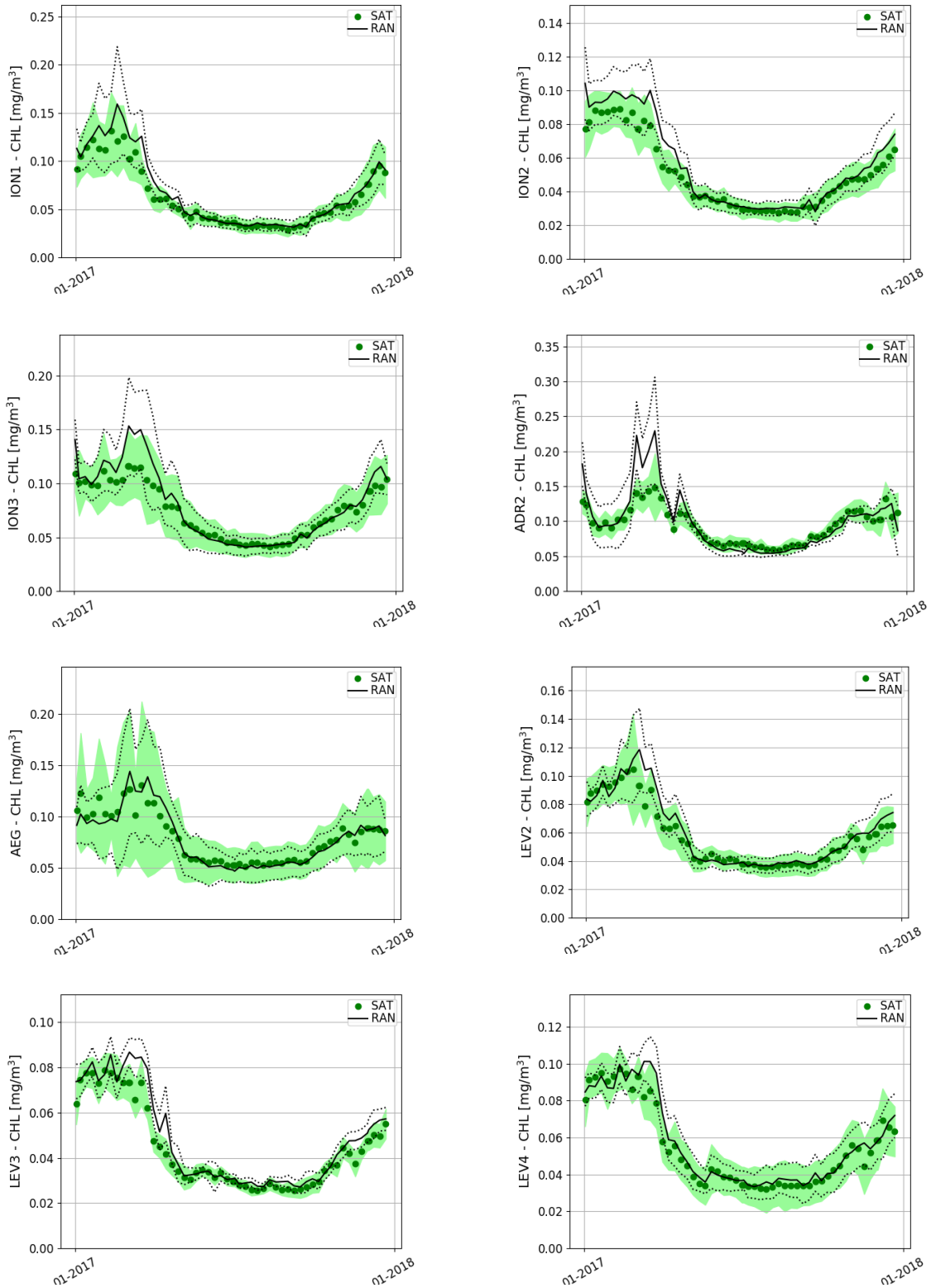

Figure IV.2. (continues) Time series of the weekly qualification run mean surface chlorophyll concentration of open sea (black solid line, RAN) with the spatial standard deviation (STD, dotted black line) and the NRT multi-sensor satellite data (green dots, SAT) with its STD (shaded green area) for 12 of the 16 sub-basins of Fig. III.1. Model data (sub-surface 0-10m layer) and satellite data are reported only for open sea areas.

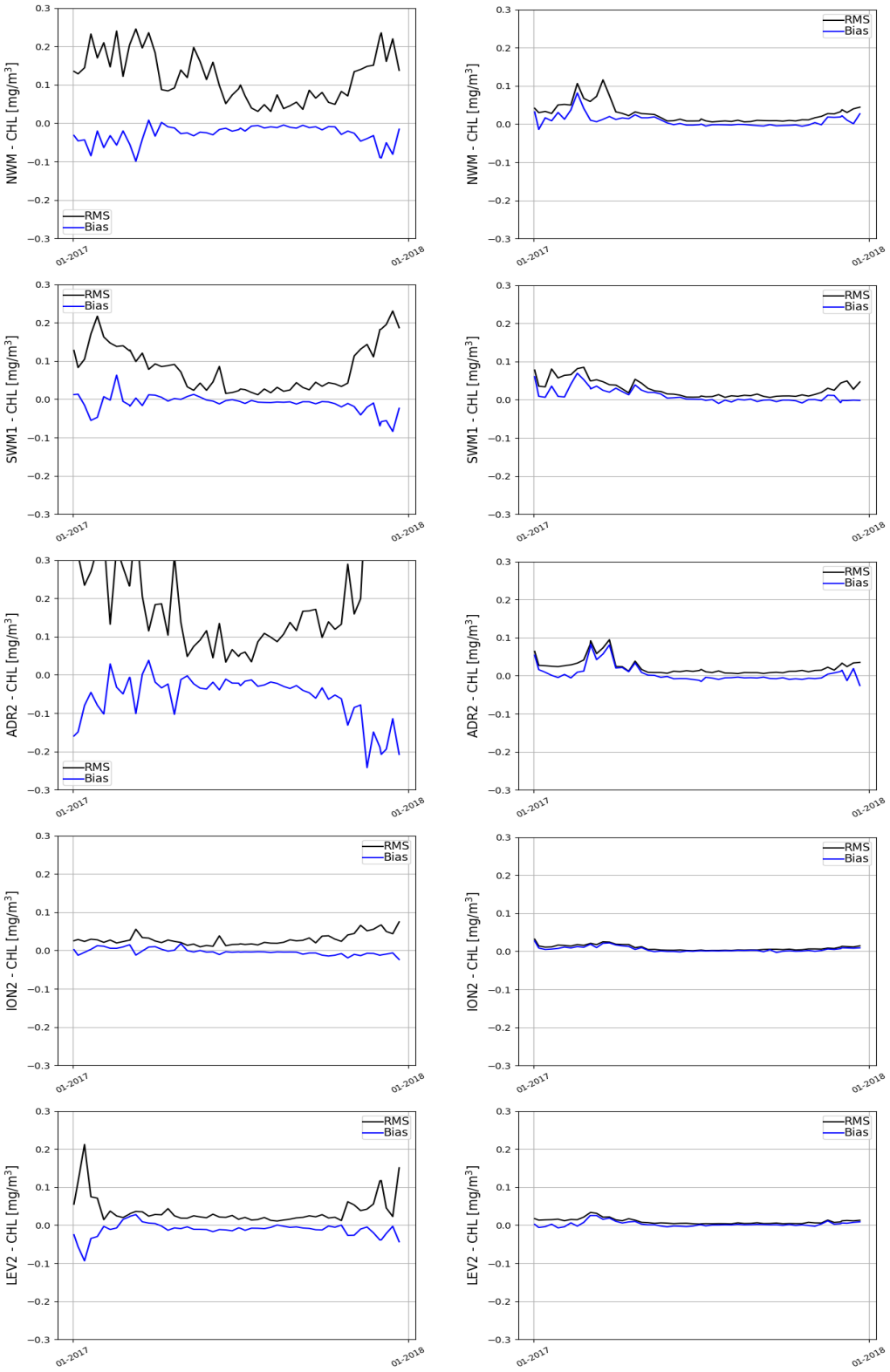

Figure IV.3. Weekly time series of BIAS (mod-ref; blue) and RMSD (black) metrics computed for 5 of the 16 Mediterranean sub-basins reported in Fig. III.1. Computation of BIAS and RMSD is based on weekly mean surface chlorophyll concentration referred to the coastal (left) and the open sea (deeper than 200 m, right) areas as shown by the Fig. III.1.

OPEN SEA	Surface (0-10m) chlorophyll Mod-Sat				Surface (0-10m) chlorophyll log_{10}(Mod)-log_{10}(Sat)			
	RMSD		BIAS		RMSD		BIAS	
	win	sum	win	sum	win	sum	win	sum
alb	0.10	0.05	0.04	0.008	0.17	0.13	0.10	0.03
swm1	0.05	0.01	0.03	<0.005	0.12	0.06	0.08	-0.005
swm2	0.05	0.006	0.03	<0.005	0.12	0.05	0.07	-0.011
nwm	0.05	0.008	0.02	<0.005	0.11	0.05	0.05	-0.016
tyr1	0.03	0.007	0.02	<0.005	0.09	0.05	0.05	-0.025
tyr2	0.03	0.005	0.02	<0.005	0.09	0.04	0.06	-0.009
adr1	0.04	0.01	0.03	-0.01	0.11	0.07	0.09	-0.063
adr2	0.04	0.01	0.03	-0.007	0.13	0.06	0.07	-0.049
aeg	0.03	0.008	<0.005	<0.005	0.09	0.05	0.01	-0.023
ion1	0.02	<0.005	0.01	<0.005	0.09	0.05	0.07	0.01
ion2	0.02	<0.005	0.01	<0.005	0.09	0.05	0.07	0.016
ion3	0.03	0.007	0.02	<0.005	0.10	0.06	0.07	-0.013
lev1	0.02	<0.005	0.01	<0.005	0.10	0.04	0.07	0.014
lev2	0.02	<0.005	0.01	<0.005	0.09	0.05	0.04	0.004
lev3	0.01	<0.005	0.01	<0.005	0.08	0.05	0.05	0.024
lev4	0.01	0.008	<0.005	<0.005	0.07	0.08	0.03	0.026
med	**0.04**	**0.01**	**0.02**	**<0.005**	**0.10**	**0.06**	**0.06**	**0.001**

Table IV.1. Mean RMSD and BIAS between surface chlorophyll model maps and satellite maps referred to open sea areas (deeper than 200 m) for the period January – December 2017. On the right side, the skill indexes are computed on the log-transformed model and satellite chlorophyll. Winter (win) corresponds to January to April, summer (sum) corresponds to June to September.

COAST	Surface (0-10m) chlorophyll Mod-Sat				Surface (0-10m) chlorophyll log_{10}(Mod)-log_{10}(Sat)			
	RMSD		BIAS		RMSD		BIAS	
	win	sum	win	sum	Win	sum	Win	sum
alb	0.17	0.06	0.01	-0.006	0.20	0.13	0.066	-0.01
swm1	0.12	0.03	<0.005	-0.007	0.15	0.09	0.04	-0.03
swm2	0.17	0.03	<0.005	-0.006	0.17	0.10	0.057	-0.03
nwm	0.17	0.07	-0.04	-0.013	0.15	0.11	<0.005	-0.03
tyr1	0.21	0.07	-0.05	-0.018	0.17	0.15	-0.02	-0.07
tyr2	0.16	0.05	-0.01	-0.011	0.17	0.12	0.03	-0.05
adr1	0.38	0.38	-0.08	-0.116	0.16	0.19	0.02	-0.12
adr2	0.25	0.10	-0.05	-0.029	0.19	0.13	0.033	-0.08
aeg	0.15	0.05	-0.02	-0.01	0.14	0.09	0.018	-0.04
ion1	0.32	0.60	-0.07	-0.148	0.16	0.23	<0.005	-0.08
ion2	0.03	0.02	0.005	-0.005	0.11	0.13	0.034	-0.03
ion3	0.08	0.02	<0.005	-0.011	0.13	0.11	0.019	-0.06
lev1	0.02	0.01	0.02	<0.005	0.15	0.12	0.117	0.03
lev2	0.05	0.02	-0.01	-0.009	0.14	0.13	-0.011	-0.06
lev3	0.59	0.52	-0.26	-0.198	0.26	0.30	-0.078	-0.14
lev4	0.32	0.29	-0.10	-0.104	0.25	0.29	-0.08	-0.16
med	**0.29**	**0.33**	**-0.05**	**-0.066**	**0.17**	**0.18**	**0.009**	**-0.07**

Table IV.2. Mean RMSD and BIAS between surface chlorophyll model maps and satellite maps referred to coastal areas (shallower than 200 m, Fig. III.1) for the period January – December 2017. On the right side, the skill indexes are computed on the log-transformed model and satellite chlorophyll. Winter (win) corresponds to January to April, summer (sum) corresponds to June to September.

The comparison of modelled chlorophyll with the BGC-Argo floats data evaluates the skill of the MedBFM model in reproducing the temporal evolution of the vertical dynamics of the phytoplankton in the Mediterranean Sea. Thus, we provide not just the *accuracy* of the CMEMS chlorophyll product (i.e., BIAS and RMSD for selected layers and sub-basins in Figure IV.5 and Table IV.3), but also the *consistency* of the MedBFM to simulate key coupled physical-biogeochemical processes is corroborated (Figures IV.4 and 6 and Table IV.4) at the mesoscale and weekly scale. This validation framework (details in Salon et al., 2019) is based on the concept of matching a BGC-Argo float profile with the corresponding (in time and space; i.e. GODAE class 4 metric) modelled profile (left column of Figure IV.4). Based on the model-float vertical match-up, specifically developed metrics are:

- surface concentration and 0-200 m vertically averaged values (upper panel on the right plots of Fig. IV.4);
- correlation between model and BGC-Argo float profiles (middle panel on the right plots of Fig. IV.4);
- thickness of the vertically mixed winter bloom (WLB, estimated between surface and the depth at which chlorophyll concentration is 10% of surface concentration during winter period) and depth of the deep chlorophyll maximum (DCM, lower panel on the right plots of Fig. IV.4).

The chlorophyll BIAS and RMSD metrics are reported as time series for selected layers and aggregated sub-basins in Figure IV.5, then averaged over year 2017 in Table IV.3. These metrics comparing model and BGC-Argo floats are reported operationally every week in the thematic regional validation webpage medeaf.inogs.it/nrt-validation, and show that the model has stable performance as long as the number of available BGC-Argo floats remains constant.

Table IV.3 shows that the RMSD is of the order of 0.03-0.04 mg/m^3 at surface and 0.05-0.08 mg/m^3 in the layer 60-100m. High uncertainty is observed in the subsurface layer because of the high variability characterizing chlorophyll dynamics at the DCM depth especially during summer (Fig. IV.5). It is worth to note that, in general, the modelled surface chlorophyll slightly overestimates the satellite data (BIAS in Table IV.1) and underestimates the BGC-Argo float data at surface (0-10m BIAS in Tab. IV.3). While this might point out an issue of consistency between the estimates of chlorophyll from satellite and BGC-Argo, it reinforces the very good performance of the MedBFM model, which lies in between the two observing systems.

As an example of the novel metrics development, the Hovmoller diagrams of chlorophyll (2nd and 3rd panels of Fig. VI.4,) show the very good qualitative agreement of the MedBFM model with the BGC-Argo floats in reproducing the temporal succession of the winter vertically mixed blooms, the onset and temporal dynamics of the deep chlorophyll maximum, and the depth of the deep chlorophyll maximum. The 4th-7th panels of Fig. IV.4 show the time series of the quantitative metrics computed on the vertical profiles comparison. The agreement between model (lines) and float (dots) at the surface, at the DCM and the 0-200 m vertical averaged chlorophyll values is pretty good (4th and 5th panels of Fig. IV.4). Correlation time series of the three floats are almost always higher than 0.7 (6th panel of Fig. IV.4). The depth of the DCM (blue line and dots in the lower panel of Fig. IV.4) is very well reproduced both in terms of vertical displacement and temporal evolution. The depth of vertical mixed winter bloom (WLB, red lines and dots in the lower panel of Fig. IV.4) is fairly good reproduced, although it is not always computable from BGC-Argo float data or model results.

Figure IV.6 summarises the new metrics in monthly time series for the aggregated sub-basins, while Table IV.4 reports the average of the time series. Statistics of the ALB, SWM and ADR sub-basins are not always reliable considering the very low number of BGC-Argo float profiles.

In fact, the number of available BGC-Argo floats measuring chlorophyll was 17 in the year 2017, and even if the use of BGC-Argo discloses new perspectives of the model validation, some cautions should be considered before generalizing the conclusions, since the relatively poor spatial coverage, the highly-varying presence of BGC-Argo floats in the sub-basins and the on-going improvement of product quality procedures of the BGC-Argo data.

Nevertheless, as a conclusion, the MedBFM model has a very high skill in reproducing the vertical dynamics of the phytoplankton chlorophyll, both considering the very high spatial heterogeneity of the Mediterranean Sea and the seasonal cycle of the coupled physical-biogeochemical processes. In particular, the correlation between vertical profiles of model and observation is up to 0.8 in all sub-basins (Fig. IV.6 and Tab. IV.4). The deep chlorophyll maximum (DCM) and winter layer bloom (WLB) positions are characterized by a mean uncertainty of 12 m and 34 m, respectively. The RMSD of the 0-200 m vertical averages is always less than 0.06 mg/m^3 in all the aggregated sub-basins.

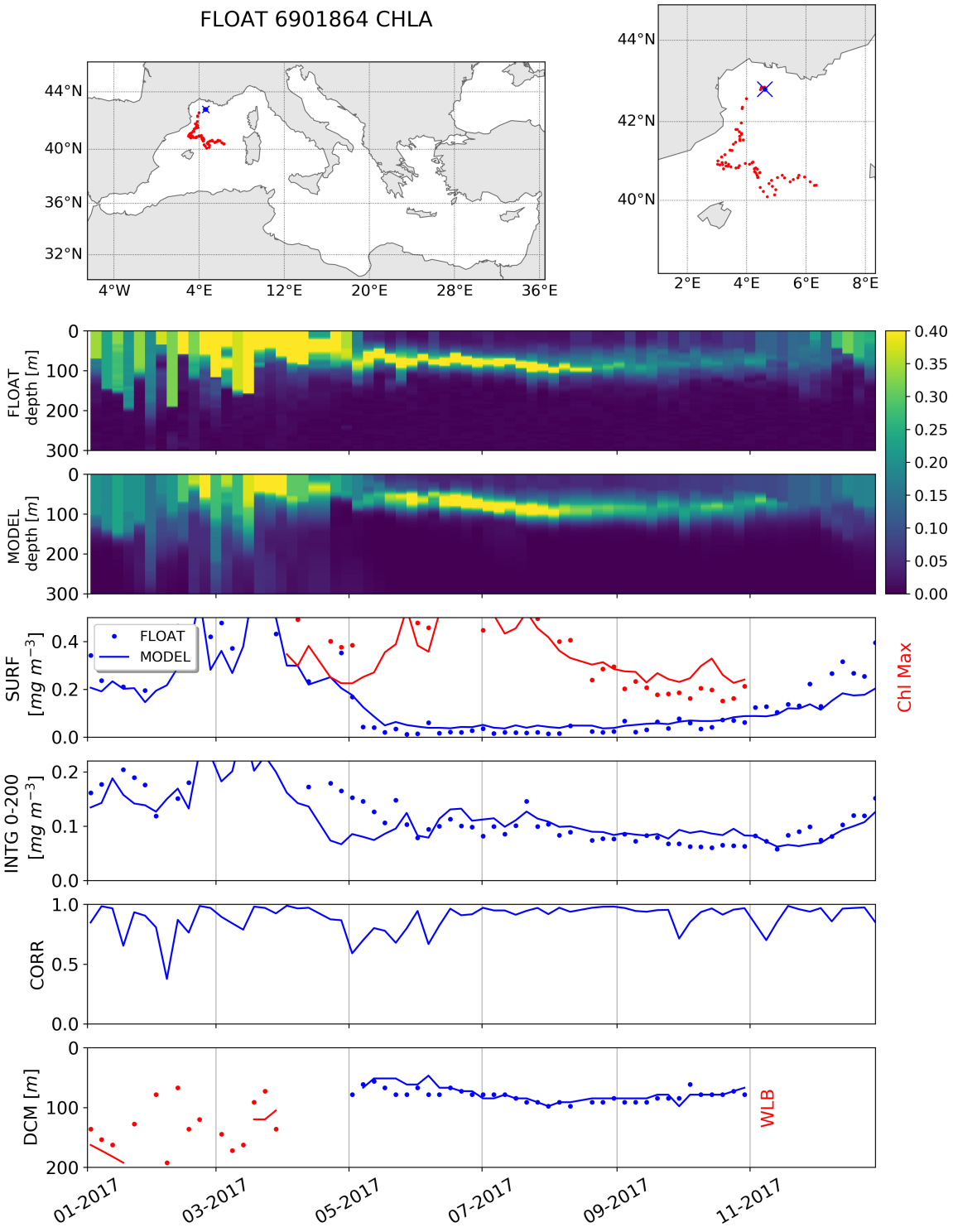

Figure IV.4. Continue overleaf.

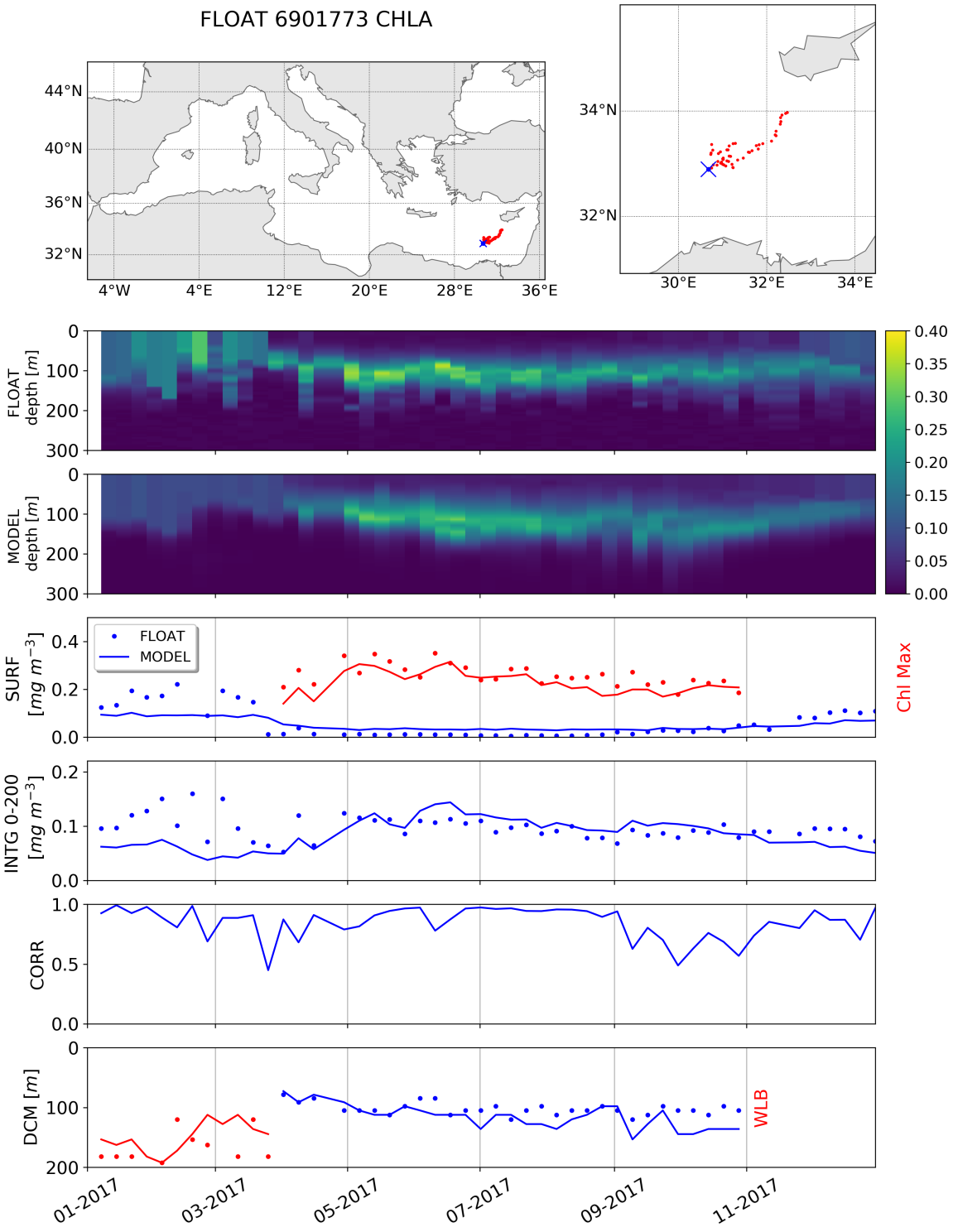

Figure IV.4. Continues overleaf.

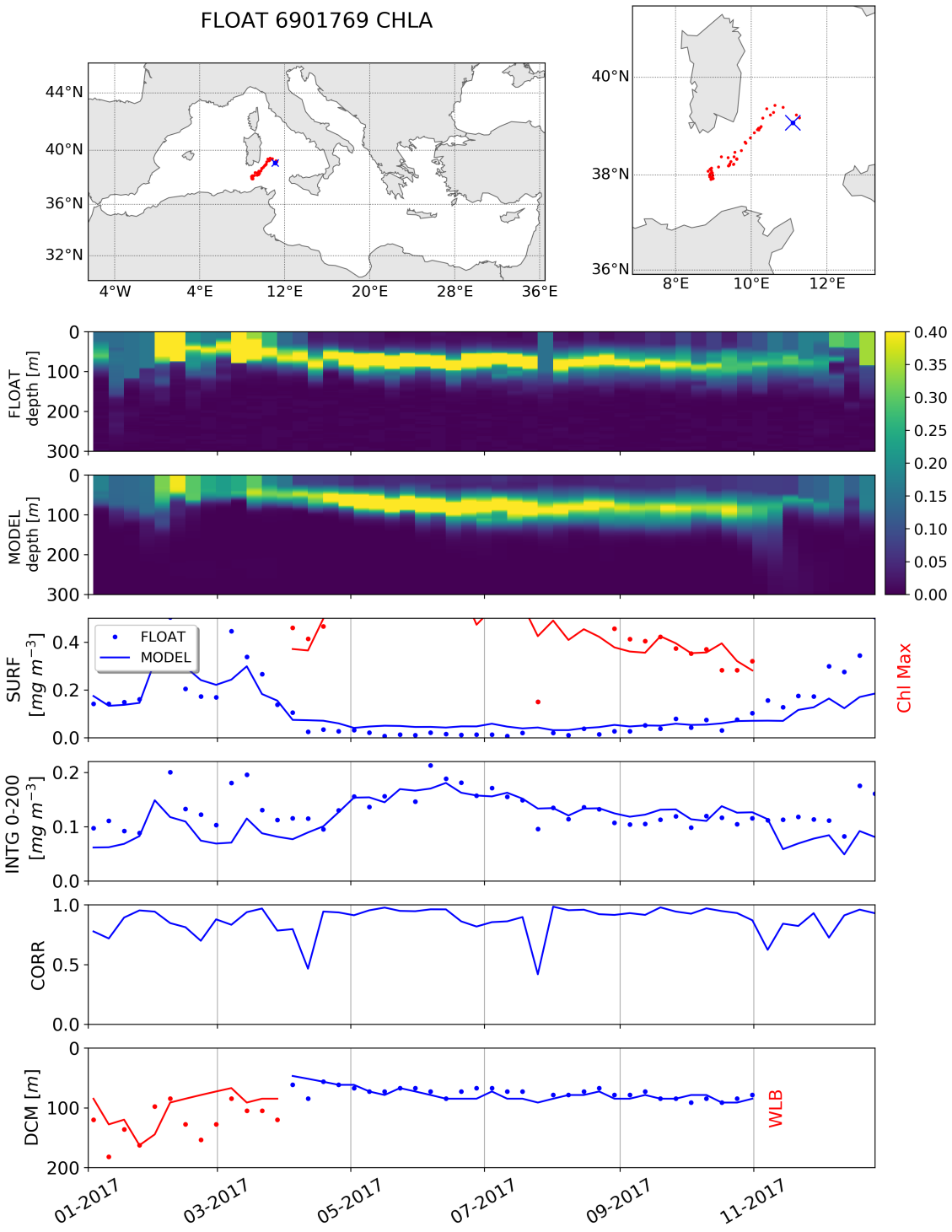

Figure IV.4. Hovmoller diagrams of chlorophyll for three selected floats (2nd panel) and the matched-up model output (3rd panel) for the year 2017, and computation of selected skill indexes for model (lines) and float data (dots). The skill indexes are: surface and value at DCM (SURF and Chl Max, 4th panel) and 0-200m vertically averaged chlorophyll (INTG, 5th panel), correlation (CORR, 6th panel), depth of the deep chlorophyll maximum (DCM, blue) and thickness of the winter layer bloom (WLB, red, 7th panel). Trajectories of the BGC-Argo floats are reported in the upper panel, with deployment position (blue cross).

Figure IV.5. Continues overleaf.

Figure IV.5. Continues overleaf.

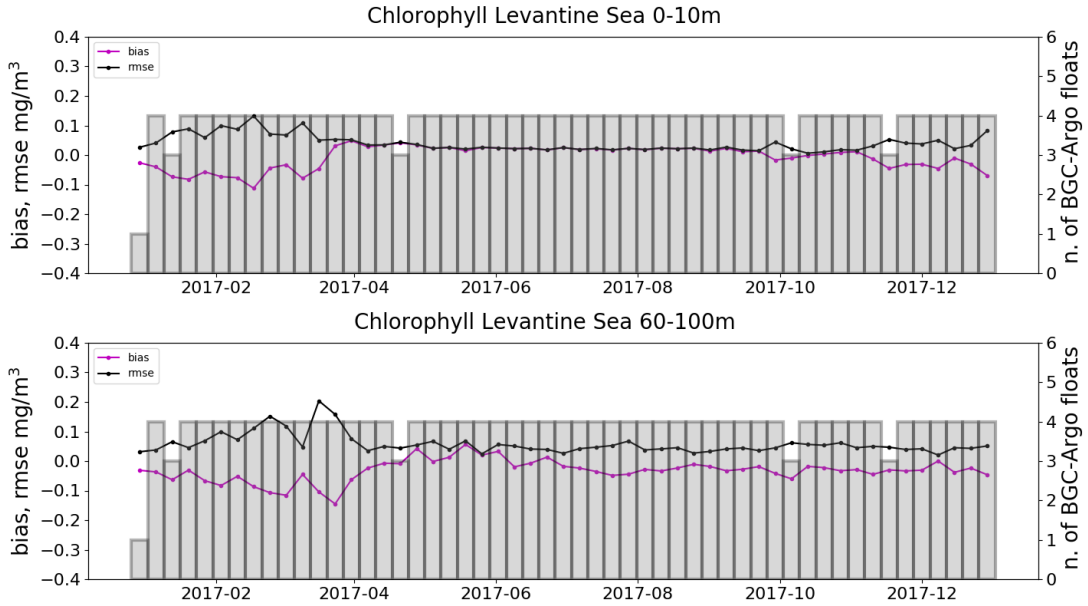

Figure IV.5. Time series of BIAS (purple) and RMSD (black) of the comparison between BGC-Argo float data and model for 0-10 m and 60-100 m layers and aggregated sub-basins (nwm, tyr = tyr1+tyr2, swm = swm1+swm2, ion = ion1+ion2+ion3, lev = lev1+lev2+lev3+lev4 of Fig. III.1). The number of data profiles used is shown with the grey vertical bars. These statistics are weekly updated in Near Real Time mode for the ANALYSIS_FORECAST product in the operational regional thematic validation website: medeaf.inogs.it/nrt-validation.

	BIAS					RMSD				
	# 0-10m	10-30m	30-60m	60-100m	100-150m	# 0-10m	10-30m	30-60m	60-100m	100-150m
alb	-	-	-	-	-	-	-	-	-	-
swm	-0.031	-0.032	-0.031	-0.001	<0.005	0.069	0.067	0.076	0.072	0.035
nwm	-0.042	-0.042	-0.041	-0.034	-0.014	0.075	0.076	0.085	0.076	0.037
tyr	-0.013	-0.018	-0.020	-0.065	<0.005	0.061	0.060	0.077	0.086	0.040
adr	0.015	0.019	0.014	0.018	0.011	0.040	0.045	0.039	0.037	0.030
ion	-0.018	-0.018	-0.018	-0.027	-0.019	0.045	0.045	0.052	0.055	0.049
lev	-0.007	-0.008	-0.015	-0.033	-0.007	0.039	0.039	0.048	0.058	0.055

Table IV.3. Time averaged BIAS and RMSD of chlorophyll (mg/m^3) for selected layers and aggregated sub-basins for the period January – December 2017. Statistics are computed using the match-ups of model with BGC-Argo float data.

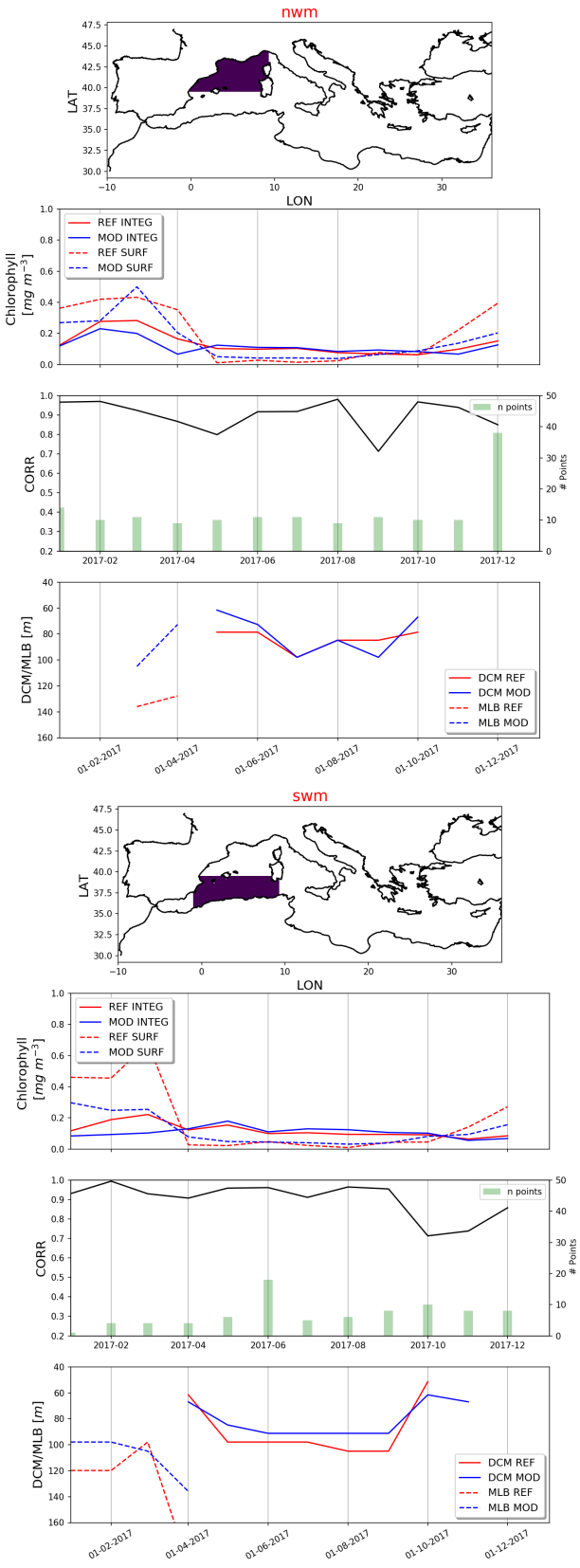
nwm
LAT
LON
REF INTEG
MOD INTEG
REF SURF
MOD SURF
Chlorophyll [mg m^{-3}]
CORR
n points
Points
DCM/MLB [m]
DCM REF
DCM MOD
MLB REF
MLB MOD
swm
LAT
LON
REF INTEG
MOD INTEG
REF SURF
MOD SURF
Chlorophyll [mg m^{-3}]
CORR
n points
Points
DCM/MLB [m]
DCM REF
DCM MOD
MLB REF
MLB MOD

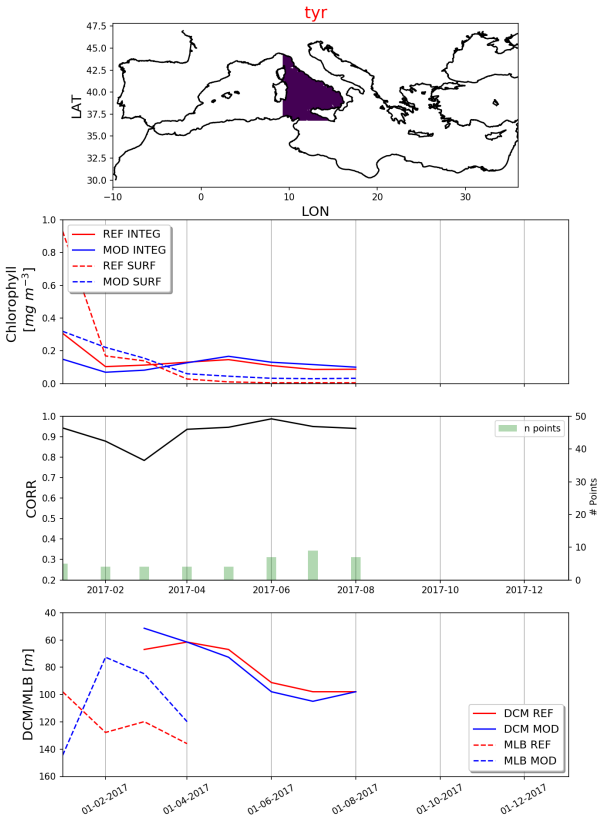

Figure IV.6. Continues overleaf.

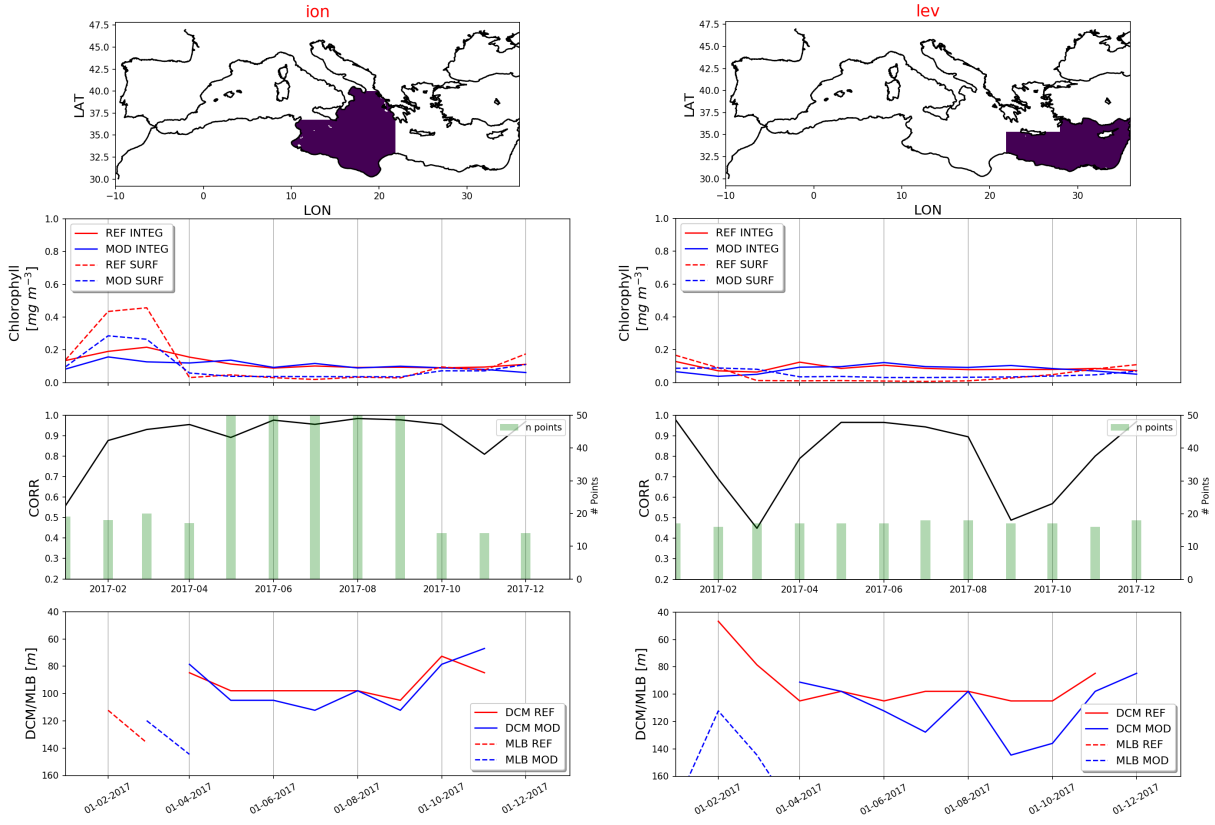

Figure IV.6. Monthly time series of chlorophyll ecosystem indicators based on the comparison between BGC-Argo float data (red lines) and model (blue lines) for aggregated sub-basins for the period January – December 2017. The ecosystem indicators are those reported in the lower panels of Fig. IV.4: vertical averaged chlorophyll (solid lines) and surface chlorophyll (dashed lines) in the upper panel, correlation (black line in middle panel), depth of the DCM (blue and red solid lines) and depth of the winter bloom layer (blue and red dashed lines) in the lower panel. The number of float profiles is reported with the green bars in the middle panel (# of float per month).

		Average 0-200 m [mg/m³]		Depth of the deep chlorophyll maximum [m]		Depth of the vertically mixed bloom in winter [m]		average number of available profiles per month
	CORR	BIAS	RMSD	BIAS	RMSD	BIAS	RMSD	
alb	-	-	-	-	-	-	-	0
swm	0.9	-0.01	0.05	-6	11	-17	29	7
nwm	0.9	-0.02	0.04	-4	10	-5	46	13
tyr	0.92	-0.02	0.06	1	8	-15	41	4
adr	0.78	0	0.02	12	13	-	-	1
ion	0.9	-0.02	0.04	2	10	-17	17	46
lev	0.79	-0.01	0.03	13	22	-29	36	17

Table IV.4. Time averages of the chlorophyll ecosystem indicators based on the BGC-Argo floats and model comparison for the period January – December 2017.

III.2 Net primary production

Net primary production (NPP) is the measure of the net uptake of carbon by phytoplankton groups (gross primary production minus fast release processes – e.g. respiration). The lack of any extensive dataset of measures of primary production prevents the application of quantitative metrics for the assessment of the quality of this product. Thus, the product quality consists in a qualitative assessment of the consistency of the modelled NPP with previous estimates published in scientific literature (Figs. IV.7 and 8 and Tab. IV.5). Simulated relevant gradients between eastern and western regions and averaged NPP in the different sub-basins are consistent with basin-wide estimates (maps from Lazzari et al., 2012 and Bosc et al., 2004) and with sub-basin averages (Tab. IV.5). Lower values in the NWM basin w.r.t. the other climatological estimates are possibly caused by the very low mixing during winter 2017 (see Ocean State Report #5 in preparation) that caused a lower-than-usual productivity for this year. The qualification run generally depicts an annual mean NPP at basin-scale within the range of the variability of the previous estimates. The monthly values computed from the MedBFM system (Fig. IV.8) are in any case consistent with the range of variability given by short period estimates reported by Siokou-Frangou et al. (2010; fifth column of Tab. IV.5).

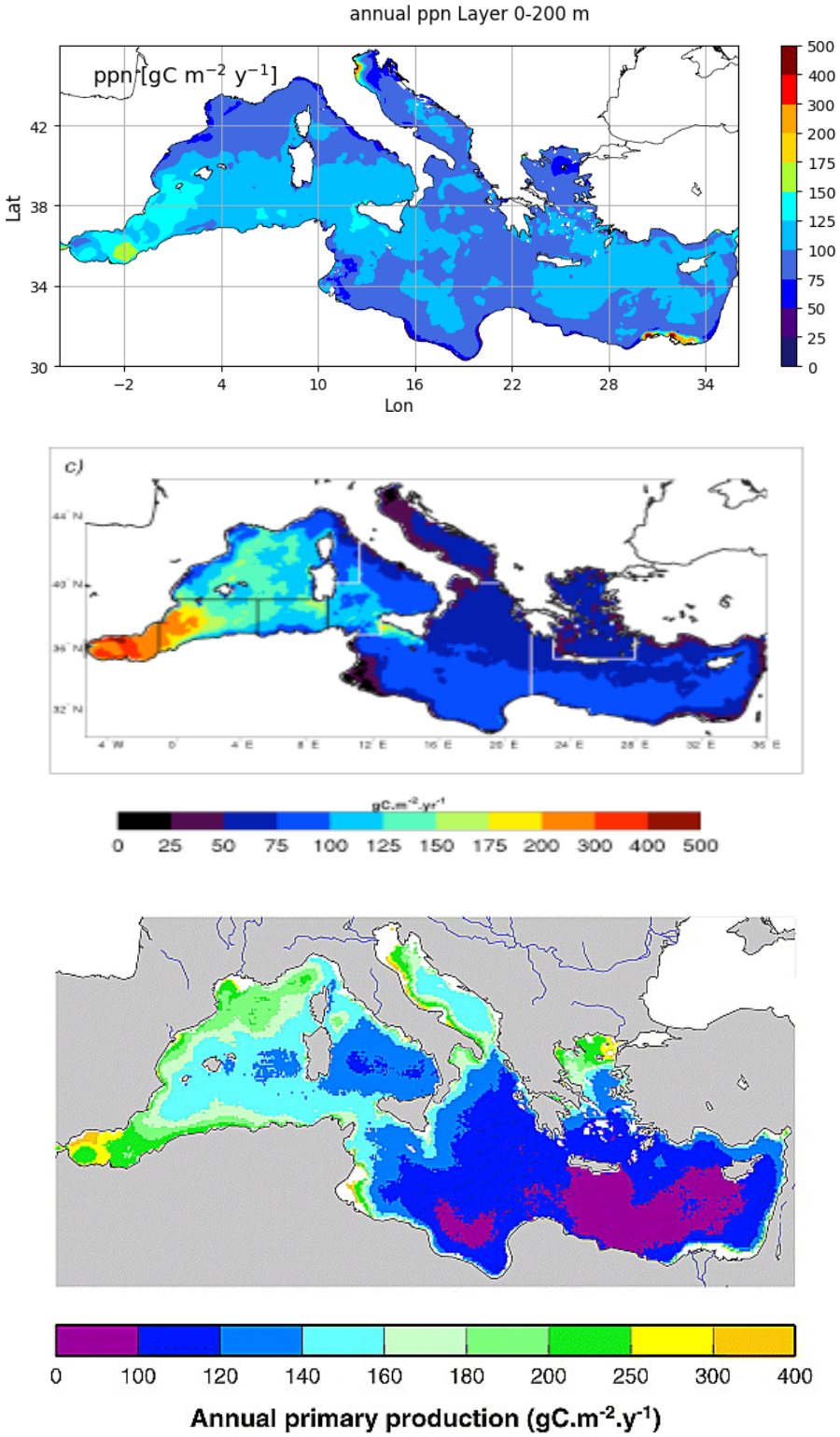

Figure IV.7. Annual averaged vertically integrated primary production (gC m^{-2} yr^{-1}) from the qualification run (average of the period January– December 2017; top panel), reference multi-annual simulation (from Lazzari et al., 2012; middle) and from satellite estimation (Bosc et al., 2004; bottom panel with different colorbar limits).

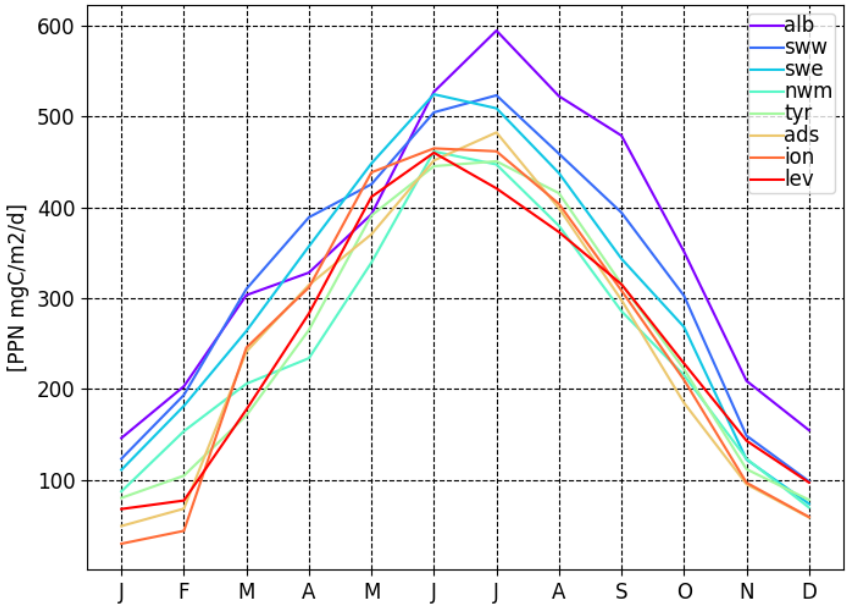

Figure IV.8. Monthly vertically integrated primary production (mgC m^{-2} d^{-1}) computed from the qualification run in the open sea areas (i.e. Jan is the average of Jan 2017, and so on).

	MODEL Lazzari et al. (2012)	SATELLITE Bosc et al. (2004)	SATELLITE Colella (2006);	IN-SITU ESTIMATES Siokou-Frangou et al., 2010		CMEMS qualification for year 2017
	Annual mean [gC/m²/y]	Annual mean [gC/m²/y]	Annual mean [gC/m²/y]	Annual mean [gC/m²/y]	Short term estimates [mgC/m³/d]	Annual mean [gC/m²/y]
Mediterranean Sea (MED)	98±82	135.5	90±48			99
Alboran Sea (ALB)	274±155	230	179±116		353–996; May-Jun1996 142; Nov2003	128
South West Med – West (SWM1)	160±89	162	113±43		186–636 (avg. 440) Oct1996	118
South West Med –East (SWM2)	118±70	162	102±38			11
North West Med (NWM)	116±79	170	115±67	105.8-119.6 86-232 (only DYFAMED station) 140-170 (South Gulf of Lion)	353–996; May–Jun1996 401; Mar-Apr1998 (G. Lion) 166; Jan-Feb1999 (G. Lion) 160–760; May-Jul (Cat-Bal) 150–900; Apr1991 (Cat-Bal) 450, 700; Jun1993 (Cat-Bal) 210, 250; Oct1992 (Cat-Bal) 1000±71 Mar1999 (Cat-Bal) 404±248 Jan-Feb00 (Cat-Bal)	91
Levantine (LEV1+LEV2+LEV3+LEV 4)	76±61	105	72±21	59 (Cretan Sea)		93
Ionian Sea (ION1+ION2+ION3)	77±58	120	79±23	61.8	119–419; May-June 1996 208–324; April-May 1999 186±65; August 1997-98	93
Tyrrhenian Sea (TYR1 + TYR2)	92±5	137	90±35		398; May–Jun1996 273; Jul2005 429; Dec2005	93

Table IV.5. Annual averages and short period estimates of the vertically integrated primary production for some selected sub-regions. Estimates are from multi-annual simulation (Lazzari et al., 2012), from satellite model (Bosc et al., 2004; Colella, 2006), from in-situ estimates (Siokou-Frangou et al., 2010) and from CMEMS V4.1 qualification run.

III.3 Phosphate and Nitrate

The quality of CMEMS Med-MFC phosphate and nitrate products is assessed in three phases:

(i) the qualitative comparison with World Ocean Atlas 2013 (WOA2013) shows the performance of reproducing basin-wide gradients (GODAE Class 1: Figs. IV.9 and 10);

(ii) the quantitative comparison with EMODnet and NODC-OGS vertical climatological profiles shows the skill in reproducing the vertical characteristics along the 16 Mediterranean sub-basins (Fig. IV.11 and Tabs. IV.6 and 7);

(iii) the quantitative comparison with BGC-Argo float illustrates the quality of the model in reproducing the nitrate dynamics at the mesoscale spatial and weekly temporal scales (Figs. IV.12, 13 and 14 and Tabs. IV.8 and 9).

The assessment of the model performance in reproducing basin-wide gradients of phosphate and nitrate is performed on a qualitatively basis by comparing the modelled maps of nutrients with the basin-wide reconstruction obtained from the WOA2013 database (1 degree horizontal resolution) at different vertical layers (Figs. IV.9 and 10). The figures show that the relevant gradients between western and eastern sub-basins and between the surface and the sub-surface layers of both phosphate and nitrate are well reproduced by the present MedBFM model.

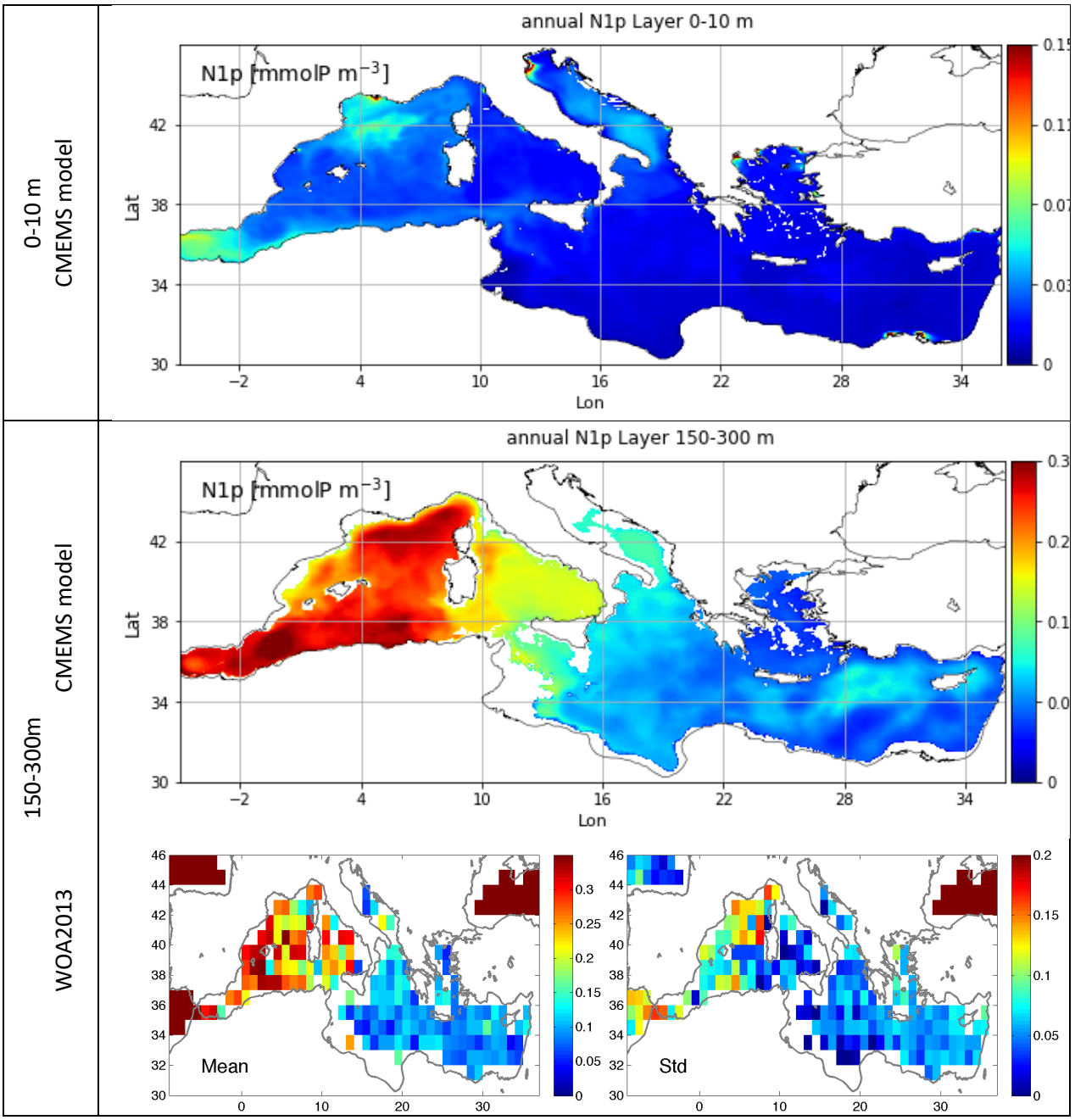

Figure IV.9. Phosphate ("N1p", mmol P/m^3) mean spatial distributions. Annual average and vertical average over the 0-10 m and 150-300 m layers from the qualification run (average of the period January - December 2017, model, top in each panel) and from WOA2013 (mean and standard deviation, bottom in each panel). The map of WOA2013 phosphate at 0-10 m is not reported since its errors are very high.

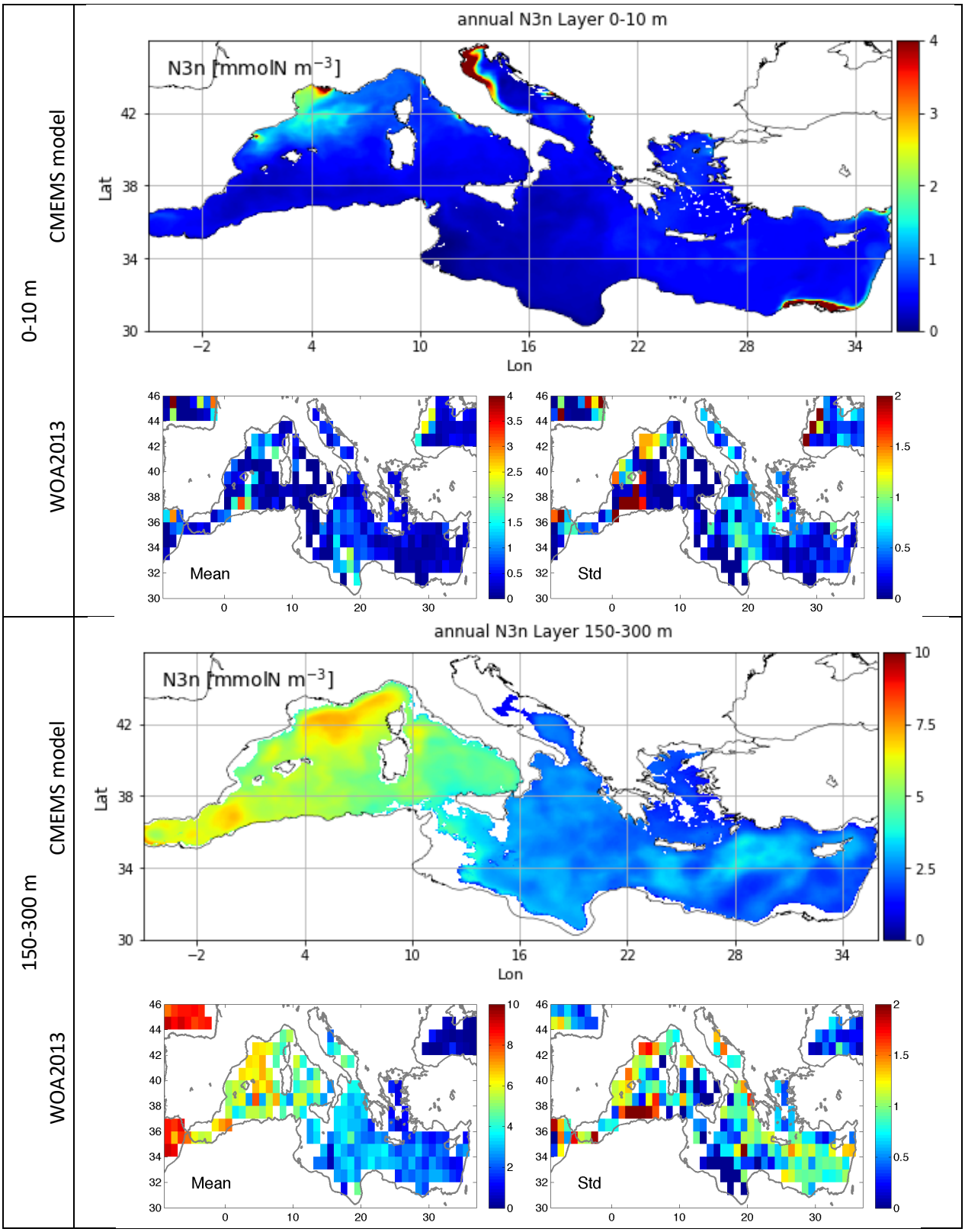

Figure IV.10. Nitrate ("N3n", mmol N/m^3) mean spatial distributions. Annual average and vertical average over the 0-10 m and 150-300 m layers from the qualification run (average of the period January - December 2017, model, top in each panel) and from WOA2013 (mean and standard deviation, bottom in each panel).

The CMEMS Med-MFC nitrate and phosphate products have a good accuracy in reproducing the average values and shape of the profiles along the Mediterranean sub-basins. In particular, the modelled profiles are within the range of variability of the NODC-OGS climatological profiles (Fig. IV.11), and the correlation values are generally larger than 0.9 (Tab. IV.7). On average, the RMSD of nitrate is 0.3-0.4 mmol/m^3 in the upper layers and around 0.7 mmol/m^3 in the layers below 60 m; absolute BIAS never exceeds 0.2 mmol/m^3 in the upper layers. Phosphate RMSD is 0.02 mmol/m^3 in the upper layers and ranges between 0.02 and 0.03 mmol/m^3 in the layers below 60m (Table IV.6). Further, Figure IV.11 shows that the model outputs are generally within the climatological variability of reference data of all sub-basins. Thus, the result corroborates the very good performance of the MedBFM model in reproducing, for both nitrate and phosphate, the deepening of the nutricline and the decreasing concentration values in the deep layers from the western to the eastern sub-basins.

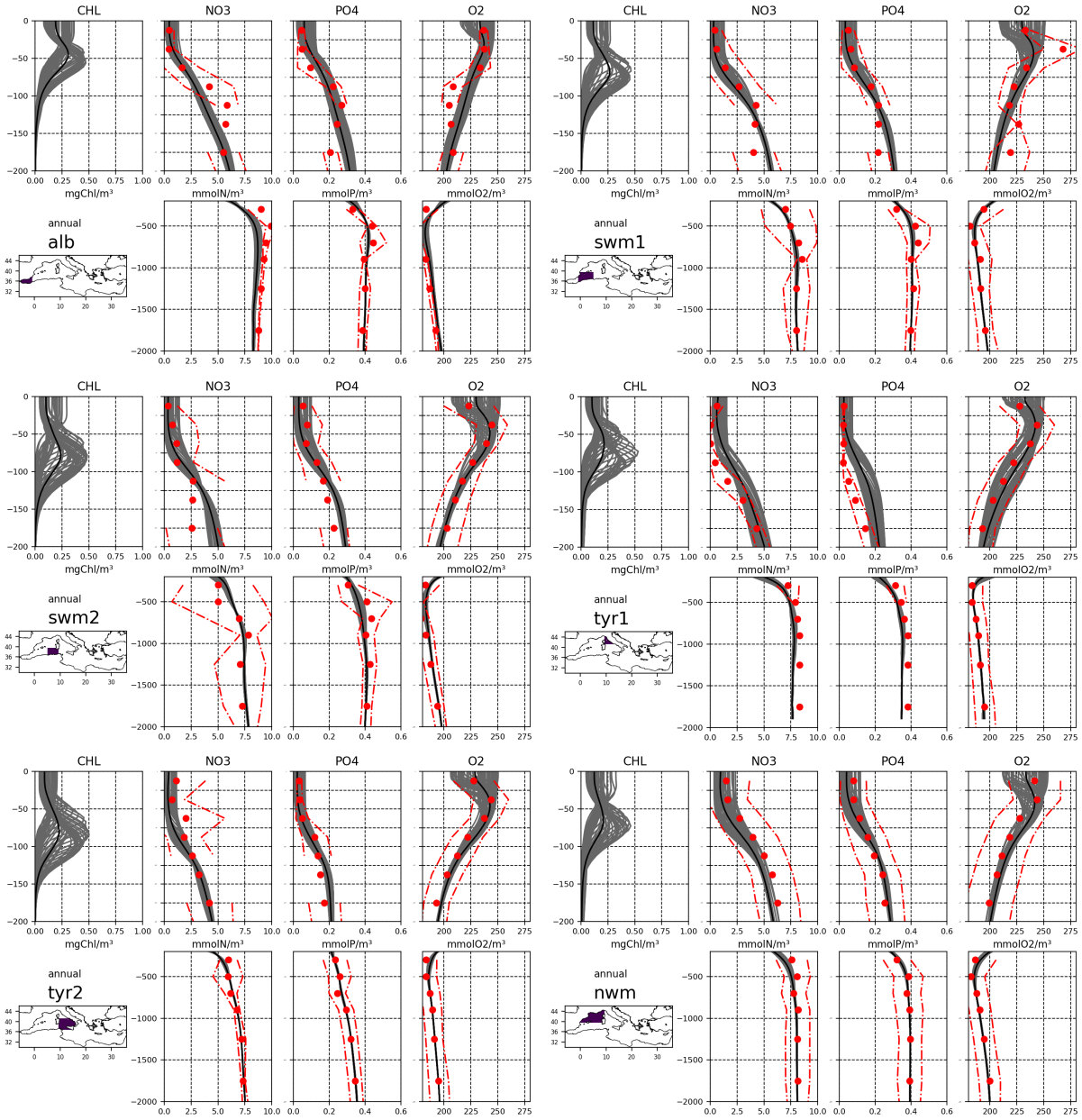

Figure IV.11. Continues overleaf.

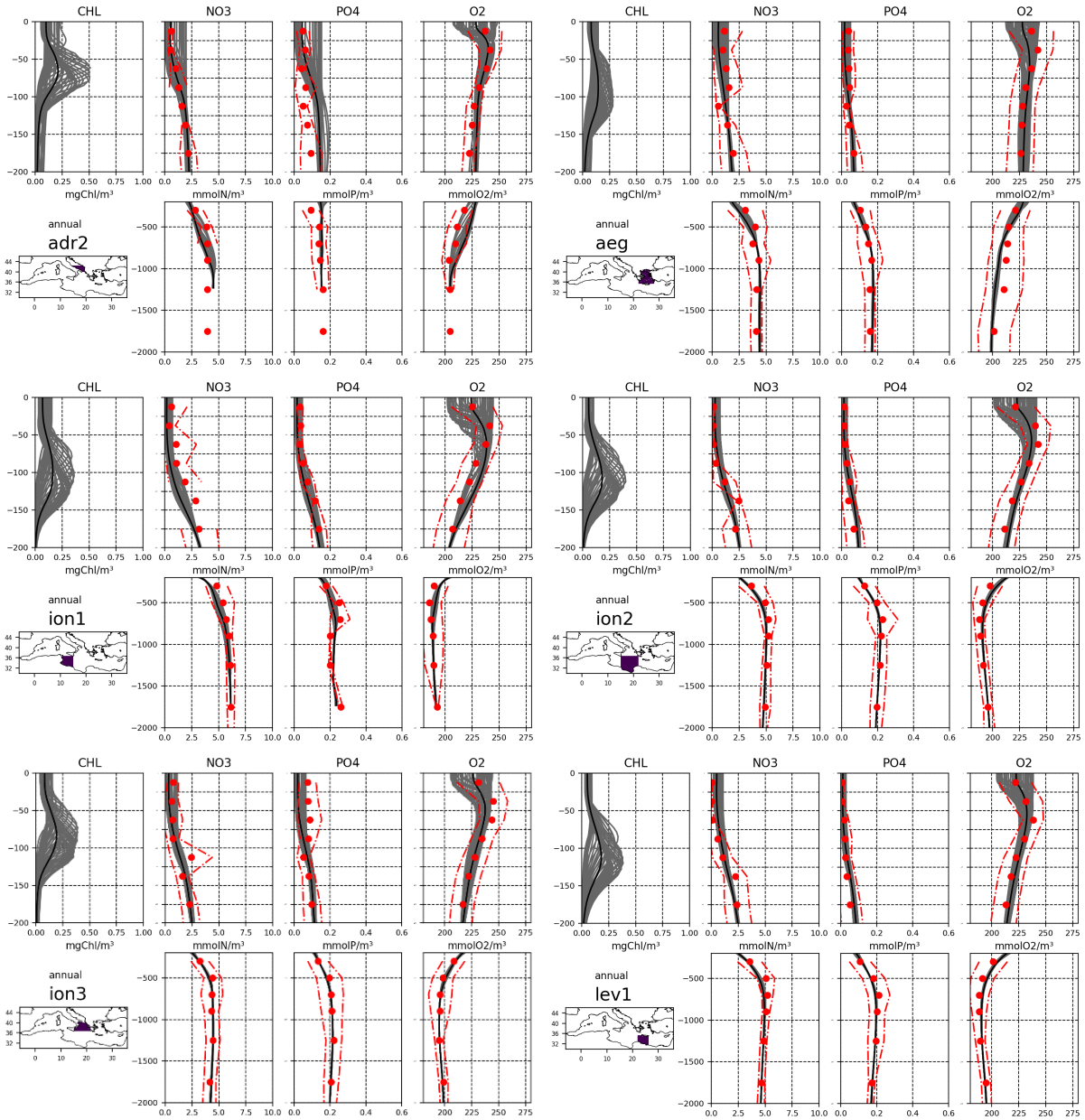

Figure IV.11. Continues overleaf.

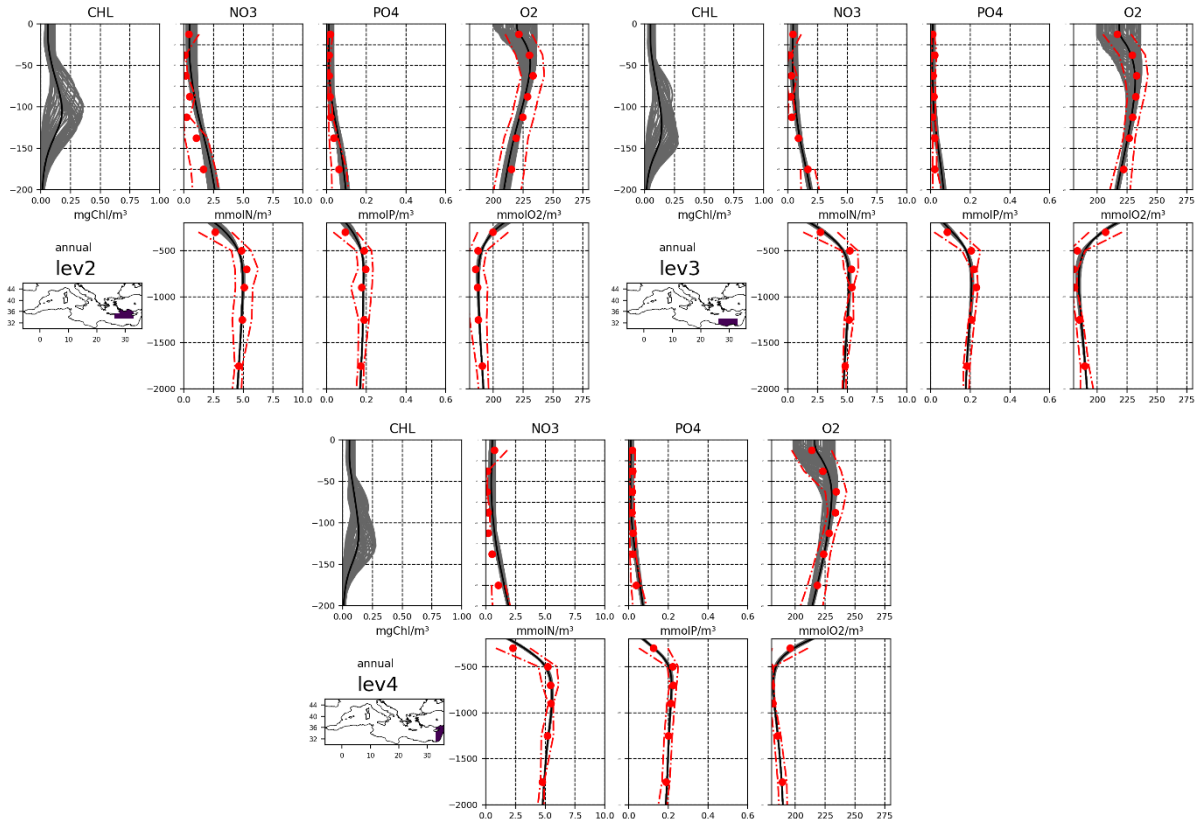

Figure IV.11. Comparison between weekly (grey lines) and annual (black lines) vertical profiles from the CMEMS model run for the Mediterranean sub-basins (except adr1 due to lack of reference data) and climatological profiles of nitrate, phosphate and dissolved oxygen retrieved from EMODnet and NODC-OGS dataset (red dots).

		0-10	10-30	30-60	60-100	100-150	150-300	300-600	600-1000
PHOSPHATE	**Bias**	-0.015	-0.012	-0.011	-0.005	0.022	0.021	-0.021	-0.009
	RMSD	0.022	0.022	0.022	0.028	0.038	0.028	0.026	0.017
NITRATE	**Bias**	-0.22	-0.05	-0.09	-0.24	0.09	-0.04	-0.50	-0.24
	RMSD	0.42	0.29	0.45	0.83	0.76	0.68	0.72	0.37

Table IV.6. BIAS and RMSD between phosphate and nitrate model outputs averaged over the sub-basins and the period January – December 2017 and the climatological vertical profiles based on the EMODnet and NODC-OGS dataset. The metric is calculated for the selected layers of Table III.1.

	alb	swm1	swm2	nwm	tyr1	tyr2	adr1	adr2	aeg	ion1	ion2	ion3	lev1	lev2	lev3	lev4
PHOSPHATE	0.97	0.98	0.98	0.99	0.96	0.99	-	0.73	0.98	0.97	0.99	0.95	0.99	0.98	0.99	0.99
NITRATE	0.98	0.99	0.97	0.99	0.99	0.99	-	0.97	0.96	0.99	0.99	0.98	0.99	0.99	1.00	0.99

Table IV.7. Mean correlation between phosphate and nitrate model profiles averaged over 2017 and climatological vertical profiles based on the EMODnet and NODC-OGS dataset for the sub-basins of Fig. III.1.

Validation of nitrate can benefit from the availability of BGC-Argo floats data. Even if the number of BGC-Argo floats mounting a nitrate sensor is smaller than that for chlorophyll (i.e., 10 BGC-Argo floats during year 2017) and the product quality activity of BGC-Argo nitrate is still under development, the float data undoubtedly represent a fundamental source of information to validate the MedBFM model results at the mesoscale and weekly scale.

The comparison of modelled nitrate with the BGC-Argo float data evaluates not just the *accuracy* of the CMEMS nitrate product (i.e., BIAS and RMSD for selected layers and sub-basins in Fig. IV.14 and Tab. IV.9), but also the *consistency* of the MedBFM to simulate key coupled physical-biogeochemical processes (i.e., water column nutrient content, nitracline and effect of winter mixing and summer stratification on the shape of nitrate profile; Figs. IV.12 and 13 and Table IV.8). This validation framework is based on matching a BGC-Argo float profile with the corresponding (in time and space) modelled profile (left column of Fig. IV.12). Based on the model-float vertical match-up, specifically developed metrics are:

- surface concentration and 0-200 m vertically averaged values (upper panel on the right plots of Fig. IV.12);
- correlation between model and BGC-Argo float profiles (middle panel on the right plots of Fig. IV.12);
- depth of the nitracline (NITRACL1 defined as the depth at which the nitrate concentration is 2 mmol/m^3; and NITRACL2 defined as the depth at which the depth derivative of the nitrate profile is maximum; lower panel on the right plots of Fig. IV.12).

The two Hovmoller plots of Fig. IV.12 exemplify the high level of potentiality of the BGC-Argo float data for validating the model results. From a qualitative point of view the nitrate signatures of all two floats are pretty well reproduced by the MedBFM model simulation (2^{nd} and 3^{rd} panel of Fig. IV.12). From a quantitative point of view the floats show a good model performance in reproducing the temporal evolution of the 0-200 m averaged values, the shape of the profile (i.e. correlation values) and of the nitracline depth (4^{th} – 7^{th} panel of Fig. IV.12).

The nitrate metrics of the 10 floats are averaged over the aggregated sub-basins in monthly time series (Fig. IV.13) and in overall means (Table IV.8). Even if the scarcity of the available floats possibly limits the generalization of the results, our validation framework highlights that the MedBFM model system shows excellent performance in simulating the shape of profiles and the seasonal evolution of the mesoscale dynamics. In particular, the mean value of nitrate on the 0-200 m layer is very well simulated, with a RMSD of the order of 0.3-0.6 mmol/m^3 (Tab. IV.8), the correlation is always higher than 0.96 and the depth of the nitracline (NITRACL1) is simulated with an uncertainty of 20 m in all aggregated subbasins (but 47m in SWM, Tab. IV.8). Further, accordingly with BGC-Argo float observations (Fig. IV.13), the MedBFM is reproducing significantly well the Mediterranean basin scale heterogeneity with a nitracline at around 80-120 m in the western sub-basins and below 120-140 m in the eastern sub-basins.

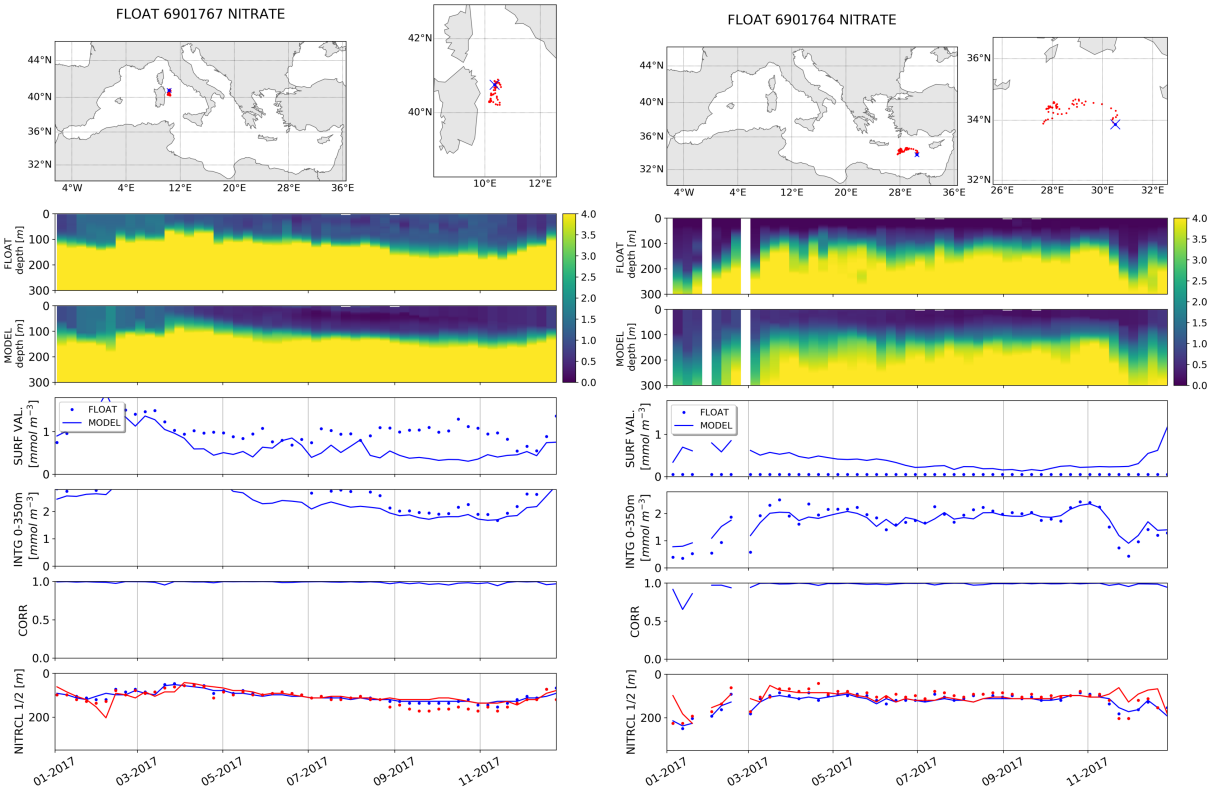

Figure IV.12. Hovmoller diagrams of nitrate of BGC-Argo floats (2nd panel) and model outputs (3rd panel) matched-up with float position (top) for year 2017. Time series of nitrate indicators based on model (MOD) and BGC-Argo floats (REF) comparison: nitrate concentration at surface (SURF, 4th panel) and 0-200m vertically averaged concentration (INTG, 5th panel), correlation between profiles (CORR, 6th panel), depth of the nitracline (NITRACL1 defined as the depth at which the nitrate concentration is 2 mmol/m^3; and NITRACL2 defined as the depth at which the depth derivative of the nitrate profile is maximum). Trajectories of the BGC-Argo floats are reported in the upper panels, with deployment position (blue cross).

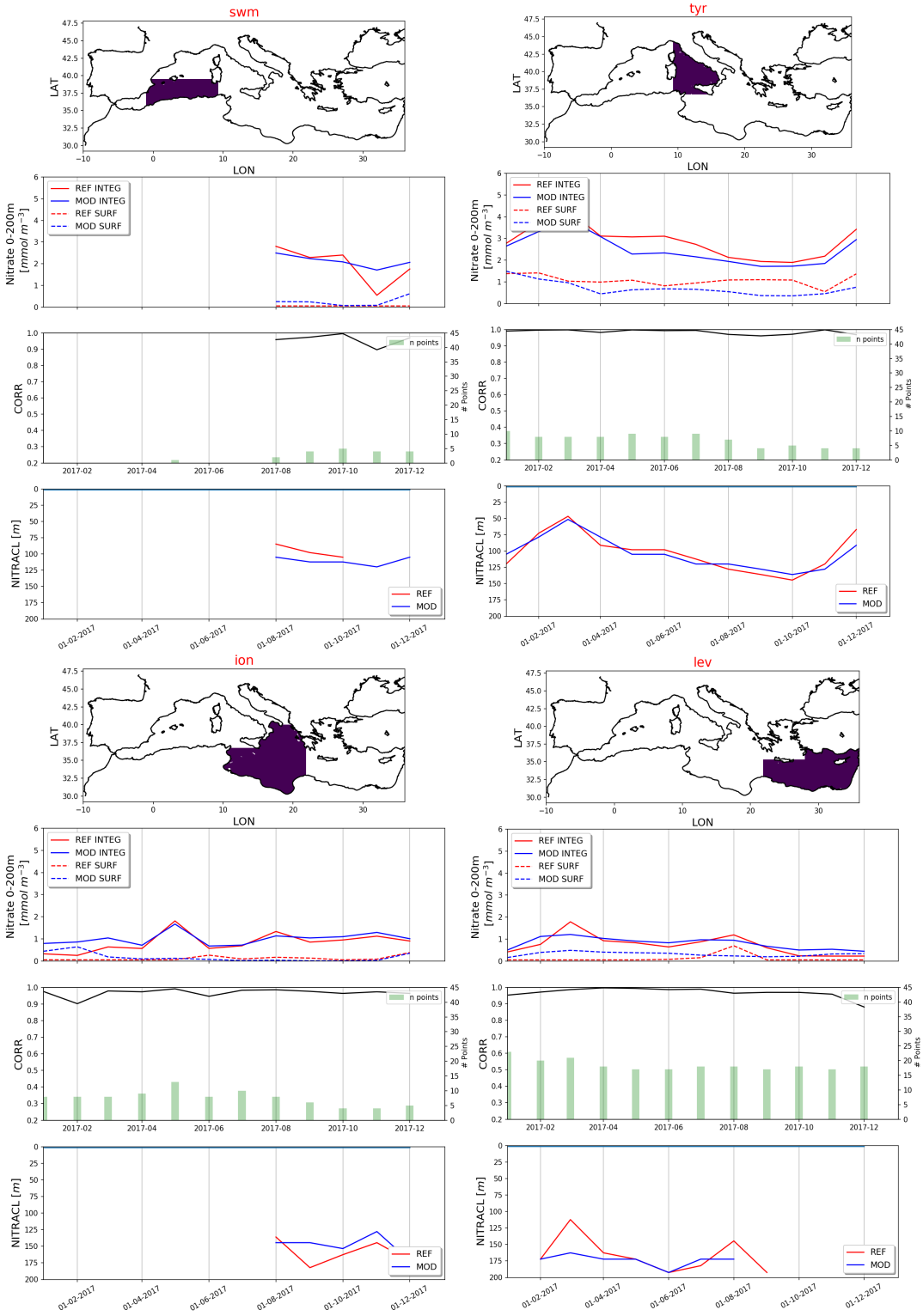

Figure IV.13. Monthly time series of nitrate indicators based on model (MOD) and BGC-Argo floats (REF) comparison for four selected aggregated sub-basins: nitrate concentration at surface (SURF) and 0-200m vertically averaged concentration (INTG), correlation between profiles (CORR), depth of the nitracline (NITRCL1). Number of float profiles is reported by the green bars in the middle panel (# of floats per month).

Finally, BIAS and RMS of nitrate concentration between model and BGC-Argo floats are computed for selected layers (listed in Table III.1) and aggregated sub-basins and they are reported as time series in Fig. IV.14 and averaged in Tab. IV.9. These metrics, which are reported and operationally updated weekly in the thematic regional validation webpage medeaf.inogs.it/nrt-validation, show that the model has stable performance as long as the number of available BGC-Argo floats remains constant (Fig. IV.14).

The availability of a sufficient number of floats equipped with the nitrate sensor might pose some issue on the reliability and sustainability of these metrics. In fact, as an example, there are no floats available in Adriatic and Alboran sub-basins in 2017 and statistics in Ionian and South Western Mediterranean sub-basins might be biased by the sparse and uneven distribution of the floats (Fig. III.4). In spite of these limitations, the metrics show that the mean RMSD is less than 0.4 mmol/m^3 in the upper 60 m and less than 0.8 mmol/m^3 in layers between 60 and 600 m (with a few exceptions).

		mean nitrate concentration 0-200m [mmol/m^3]		Depth of the nitracline [m]		Average number of profiles per month
	CORR	BIAS	RMSD	BIAS	RMSD	
alb	-	-	-	-	-	0
swm	0.96	0.11	0.53	5	16	2
nwm	0.96	0.4	0.63	-33	47	4
tyr	0.99	-0.38	0.44	1	11	7
adr	-	-	-	-	-	0
ion	0.97	0.17	0.28	-8	18	8
lev	0.97	0.08	0.26	11	22	18

Table IV.8. Averages of the monthly nitrate indicators plotted in Figure IV.13 during the period January – December 2017. The indicators are the correlation between model and BGC-Argo float data, the BIAS and RMSD of the vertically 0-200 m averaged nitrate concentration, the BIAS and RMSD of the depth of the nitracline (depth of nitrate concentration reaching 2 mmol/m^3). Statistics are computed for selected aggregated sub-basins.

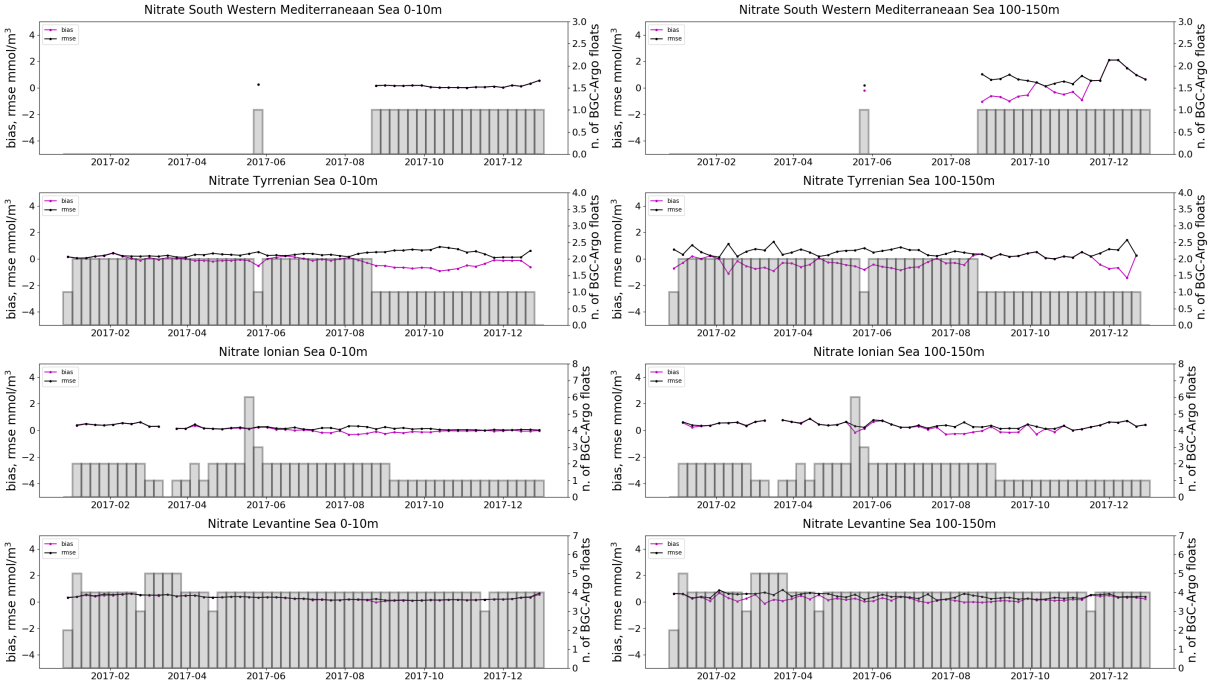

Figure VI.14. Time series of BIAS (purple) and RMSD (black) of nitrate concentration [mmol/m^3] of the comparison between BGC-Argo float data and model for the 0-10m (left) and 100-150m (right) layers and 4 aggregated sub-basins (swm, tyr = tyr1+tyr2, ion = ion1+ion2+ion3, lev = lev1+lev2+lev3+lev4 of Fig. III.1). Number of data profiles used is shown by the grey vertical bars. These statistics are updated every week in the operational regional thematic validation website: medeaf.inogs.it/nrt-validation.

	BIAS								RMSD							
	0-10m	10-30m	30-60m	60-100m	100-150m	150-300m	300-600m	600-1000m	0-10m	10-30m	30-60m	60-100m	100-150m	150-300m	300-600m	600-1000m
alb	-	-	-	-	-	-	-	-	-	-	-	-	-	-	-	-
swm	0.15	0.10	-0.23	-0.30	0.11	0.07	-0.71	-0.817	0.15	0.12	0.28	0.54	0.78	0.29	0.82	0.81
nwm	0.40	0.37	0.20	0.32	0.46	0.20	0.92	0.21	0.40	0.37	0.35	0.53	0.67	0.30	0.98	0.26
tyr	-0.19	-0.21	-0.34	-0.48	-0.25	-0.18	0.11	-1.08	0.37	0.36	0.42	0.59	0.49	0.291	0.53	1.14
adr	-	-	-	-	-	-	-	-	-	-	-	-	-	-	-	-
ion	0.07	0.05	0.05	0.20	0.30	0.14	-0.79	-1.35	0.20	0.21	0.20	0.25	0.41	0.33	0.84	1.35
lev	0.29	0.28	0.21	0.18	0.21	-0.07	-0.91	-0.89	0.32	0.30	0.25	0.28	0.44	0.44	1.08	0.94

Table IV.9. Averaged BIAS and RMSD of nitrate w.r.t. BGC-Argo floats for the layers of Tab. III.1, aggregated sub-basins (nwm, swm = swm1+sm2, tyr = tyr1+tyr2, ion = ion1+ion2+ion3, lev = lev1+lev2+lev3+lev4) for the period January – December 2017.

III.4 Dissolved Oxygen

The quality of CMEMS Med-MFC dissolved oxygen is assessed in two phases:

(i) the quantitative comparison with EMODnet and NODC-OGS vertical climatological profiles shows the skill in reproducing the vertical characteristics along the 16 Mediterranean sub-basins (Fig. IV.11 and Tabs. IV.10 and 11);

(ii) the quantitative comparison with BGC-Argo float illustrates the quality of the model in reproducing the oxygen dynamics at the mesoscale spatial and weekly temporal scales (Figs. IV.15 and 16 and Tabs. IV.12).

Modelled oxygen profiles are well within the range of variability of the climatology (Fig. IV.11; see also the very high correlation values in Table IV.11), with absolute BIAS and RMSD lower than 6 mmol/m^3 in all selected layers (Tab. IV.10).

DISSOLVED OXYGEN	0-10m	10-30m	30-60m	60-100m	100-150m	150-300m	300-600m	600-1000m
BIAS	0.40	-1.32	-3.73	1.62	2.41	0.67	6.10	1.70
RMSD	4.94	5.04	5.83	6.11	4.73	4.32	6.73	3.51

Table IV.10. BIAS and RMSD between dissolved oxygen model outputs averaged over the period January – December 2017 and climatological vertical profiles based on the EMODnet and NODC-OGS dataset. The metrics are calculated for the selected layers of Table III.1.

DISSOLVED OXYGEN	alb	swm1	swm2	nwm	tyr1	tyr2	adr1	adr2	aeg	ion1	ion2	ion3	lev1	lev2	lev3	lev4
Correlation	0.96	0.94	0.99	0.97	-	0.99	-	0.95	0.94	0.97	0.98	0.99	0.99	1.00	1.00	0.99

Table IV.11. Mean correlation between dissolved oxygen model profiles averaged over the period January – December 2017 and climatological vertical profiles based on the EMODnet and NODC-OGS dataset for the sub-basins of Fig. III.1.

The validation of dissolved oxygen can benefit from the availability of BGC-Argo float data. However, there are some issues that prevent the full exploitation of this very important source of data. The product quality activity of dissolved oxygen is still under development, and only few floats include the intercalibration in air (Bittig et al., 2019). Therefore, oxygen data from BGC-Argo floats might be affected by systematic biases. Given these limitations, the present validation framework aims at showing the potentiality of the use of BGC-Argo float data. Figure IV.15 shows the Hovmoller diagram of one selected BGC-Argo float and the corresponding model profiles along the trajectory covered by the floats. The MedBFM simulates, consistently with the BGC-Argo float data, the seasonal evolution of the oxygen, reproducing the mixed water column in winter and the formation of a maximum oxygen layer in correspondence of the DCM during summer and the depletion of the oxygen content at surface during summer.

Figure IV.16 reports the time series of the BIAS and RMSD metrics computed in the layers and aggregated sub-basins, and Table IV.12 reports their averages showing a mean absolute BIAS of 16 mmol/m^3 and a mean RMSD of 19 mmol/m^3 (with values ranging between 9 and 30 mmol/m^3) depending on the layer and sub-basins. The time series of Fig. IV.16 displaying that BIAS and RMSD are reported and

operationally updated weekly in the thematic regional validation webpage medeaf.inogs.it/nrt-validation.

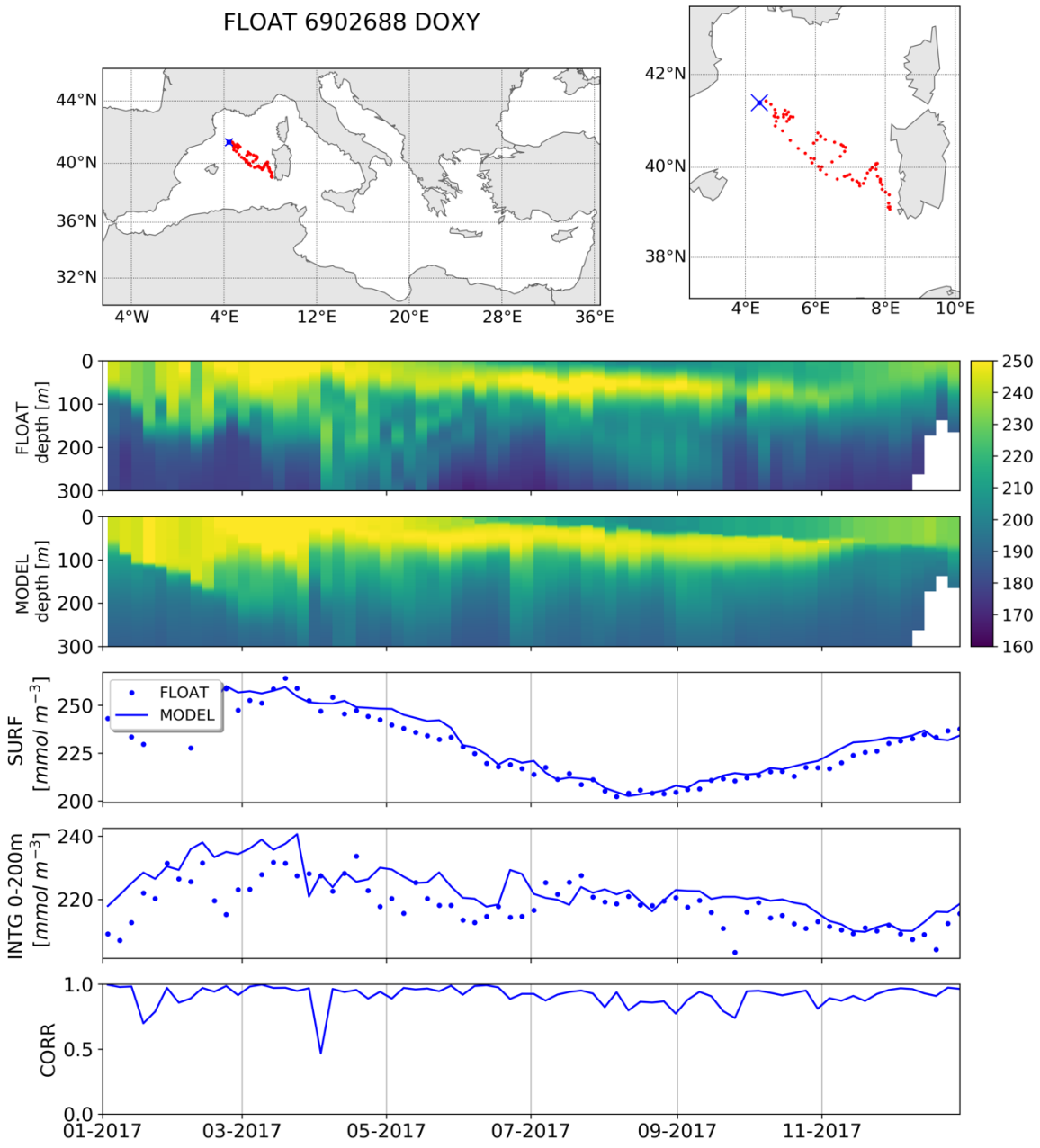

Figure IV.15. Hovmoller diagrams of dissolved oxygen of a BGC-Argo float (2nd panel) and model outputs (3rd panel) matched-up with the float data position for the year 2017. Time series of oxygen indicators based on model (MOD) and BGC-Argo floats (FLOAT) comparison: oxygen concentration at surface (SURF, 4th panel) and 0-200m vertically averaged concentration (INTG, 5th panel), correlation between profiles (CORR, 6th panel). The trajectory of the BGC-Argo float is reported in the upper panels, with deployment position (blue cross).

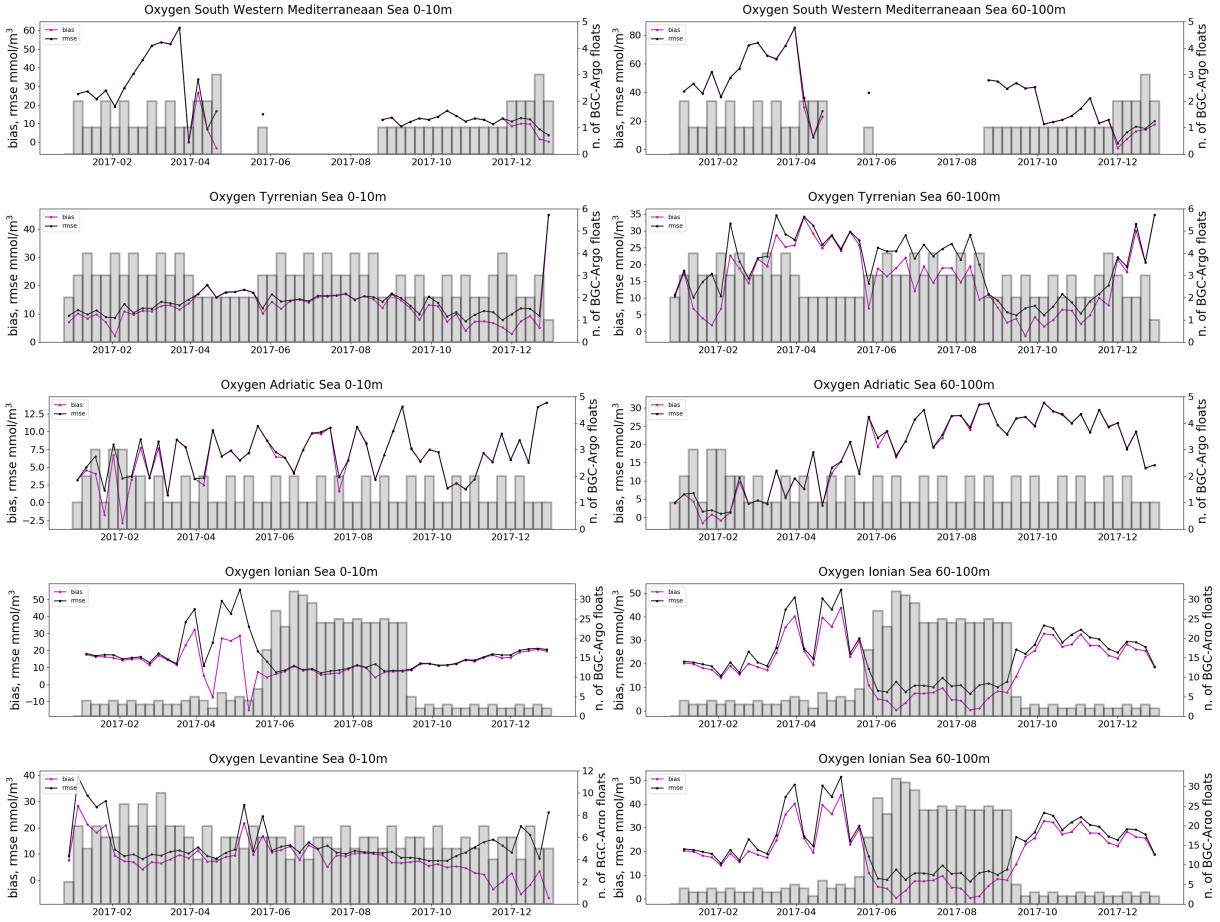

Figure VI.16. Time series of dissolved oxygen BIAS and RMSD [mmol/m^3] of the comparison between BGC-Argo float data and model for 0-10m (left) and 60-100m (right) layers and the aggregated sub-basins (adr = adr1+adr2, ion = ion1+ion2+ion3, lev = lev1+lev2+lev3+lev4, swm, tyr = tyr1+tyr2, of Fig. III.1). Number of data profiles used is shown by the grey vertical bars. These statistics are weekly updated in Near Real Time mode for the analysis and forecast product in the operational regional thematic validation website: medeaf.inogs.it/nrt-validation.

	BIAS								RMSD							
	0-10m	10-30m	30-60m	60-100m	100-150m	150-300m	300-600m	600-1000m	0-10m	10-30m	30-60m	60-100m	100-150m	150-300m	300-600m	600-1000m
alb	19.46	20.78	23.77	37.90	35.41	28.40	25.49	24.06	20.70	22.46	25.23	38.62	36.46	28.60	25.51	24.06
swm	8.39	7.02	10.11	13.53	11.52	13.55	17.78	16.43	11.48	11.09	12.96	17.77	17.61	17.90	19.14	17.71
nwm	12.55	10.57	8.59	15.66	15.19	12.95	15.34	20.80	14.09	12.81	14.24	19.80	18.71	14.90	17.12	21.40
tyr	6.46	4.84	9.60	18.08	19.03	1.14	-3.76	-2.93	6.86	6.67	10.39	18.42	19.32	3.00	7.00	2.95
adr	12.55	11.90	11.89	19.26	21.52	19.58	20.82	20.60	17.14	16.10	18.27	23.04	24.00	21.96	22.85	22.78
ion	8.24	7.16	7.43	10.83	13.26	12.83	14.64	15.39	13.57	12.44	13.37	16.10	18.00	17.64	20.181	17.42
lev	19.46	20.78	23.77	37.90	35.41	28.40	25.49	24.06	20.70	22.46	25.23	38.62	36.46	28.60	25.51	24.06

Table IV.12. Averaged dissolved oxygen BIAS and RMSD of the comparison between BGC-Argo float and model values for the layers of Tab. III.1 and aggregated sub-basins of Fig. III.1.

III.5 pH and pCO2

Variables of the carbonate system, DIC (dissolved inorganic carbon), pH (ocean acidity in total scale at insitu conditions) and pCO2 (partial pressure of carbon dioxide in sea water), along with Alkalinity (i.e., the other master variable of the carbonate system) have been validated using a climatology derived from the CarbSys datasets of Table III.3 and Fig. III.3.

Considering the availability of historical observations (section III), two climatological reference datasets have been computed: mean annual climatological maps at 1°x1° of resolution for the layers of Table III.1 (first three layers 0-10, 10-30 and 30-60 have been merged), and mean vertical profiles computed over the sub-basin of Fig. III.1. Model results (January – December 2017) are aggregated to the corresponding vertical and horizontal discretization and skill performance metrics are computed.

Vertical profiles for pH in total scale, pCO2, DIC and ALK are reported in Fig. IV.17 showing the good performance of the model in reproducing the vertical structures of carbonate system variables along the Mediterranean sub-basins, with the model vertical profiles well within the range of variability of climatological profiles. The skill metric values (i.e. BIAS, RMS and correlation between model and climatological profiles in Tab. IV.13) confirm the satisfactory skill of the MedBFM model in reproducing the average conditions of the carbonate system variables at the basin scale. In particular, the averaged RMSDs over the 16 sub-basins are around 12-14 µmol/kg for ALK and DIC, 0.015 for pH and 24 µatm for pCO2. The correlations of ALK and DIC are very high for most of the sub-basins. In some areas (i.e. lev1, lev2, lev3 and lev4) correlation of ALK is low due to the very straight shape of the profiles in eastern Mediterranean. It is worth to remind that pCO2 and pH are diagnostic variables of the model, which depends on carbonate system thermodynamics equilibrium and solubility calculation. Thus, DIC and alkalinity (i.e., the usually observed variables) are the most reliable variables to investigate the carbonate system dynamics.

	ALK [µmol/kg]			DIC [µmol/kg]			pH in total scal			pCO2 [µatm]		
Sub-basins	**BIAS**	**RMS**	**CORR**	**BIAS**	**RMS**	**CORR**	**BIAS**	**RMS**	**CORR**	**BIAS**	**RMS**	**CORR**
alb	5.87	13.76	0.99	3.41	18.25	0.98	0.004	0.016	0.62	9.8	21.7	0.78
swm1	7.34	13.53	1.00	7.46	16.59	0.99	-0.009	0.019	0.78	29.9	35.3	0.66
swm2	1.91	6.62	0.99	5.67	13.11	0.99	-0.003	0.012	0.93	28.1	28.8	0.98
nwm	-7.88	11.56	0.95	-8.93	14.15	0.90	0.001	0.01	0.94	17.5	20.7	0.53
tyr1	-	-	-	-	-	-	-	-	-	-	-	-
tyr2	0.33	11.05	0.95	0.27	15.37	0.95	-0.001	0.011	0.90	19.5	23.8	0.61
adr1	-2.98	6.23	0.56	-21.10	22.50	0.83	0.002	0.024	-0.61	15.1	26.7	-0.54
adr2	6.25	9.82	0.31	1.82	8.44	0.82	0	0.012	0.50	15.9	20.6	0.25
aeg	-17.52	22.97	0.81	-3.86	8.30	0.84	-0.018	0.032	0.60	42.8	46.5	-0.08
ion1	1.82	10.98	0.92	-1.23	14.29	0.92	0.007	0.017	0.76	11.9	25.8	0.62

ion2	4.88	10.59	0.90	7.51	11.72	0.98	-0.007	0.016	0.81	25.7	29.9	0.91
ion3	-4.75	12.55	0.70	-7.35	15.37	0.68	0	0.013	0.74	18.0	22.4	0.32
lev1	8.27	13.81	-0.16	5.56	15.68	0.80	0.007	0.012	0.84	9.7	14.2	0.80
lev2	5.49	8.50	0.62	3.34	8.04	0.95	0.01	0.012	0.94	1.1	13.5	0.97
lev3	7.02	14.04	-0.26	6.10	13.86	0.79	0.003	0.007	0.95	14.9	17.0	0.98
lev4	8.80	14.56	0.39	8.76	13.39	0.92	-0.003	0.009	0.93	25.3	27.2	0.94
average	**1.66**	**12.04**	**0.64**	**0.49**	**13.94**	**0.89**	**<0.001**	**0.015**	**0.71**	**19.0**	**24.9**	**0.58**

Table IV.13. Skill metrics of the comparison between model and climatological profiles of ALK, DIC, pCO2and pH in total scale on the selected sub-basins. Statistics are computed using model output of the period January - December 2017.

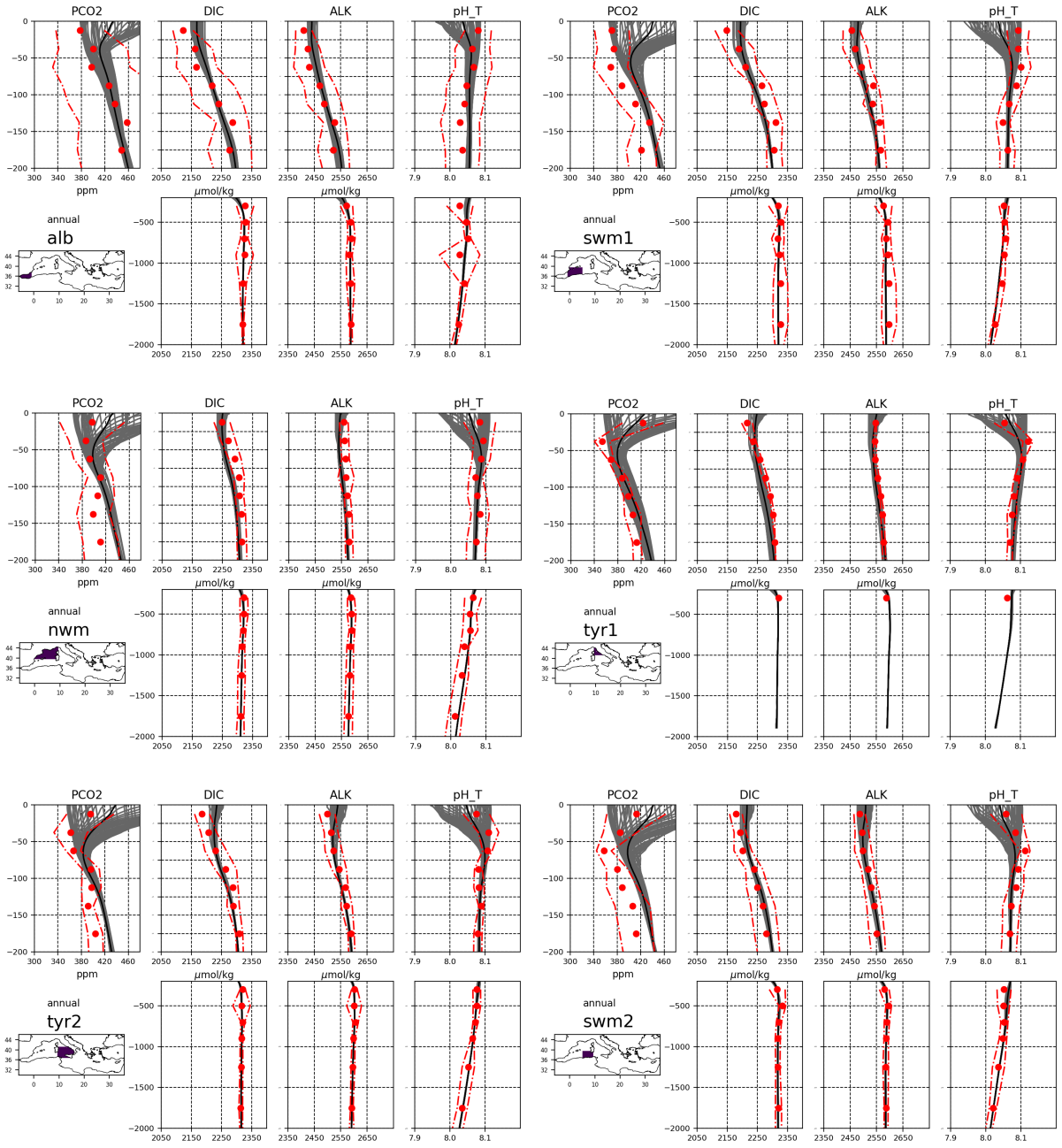

Figure IV.17. Continues overleaf.

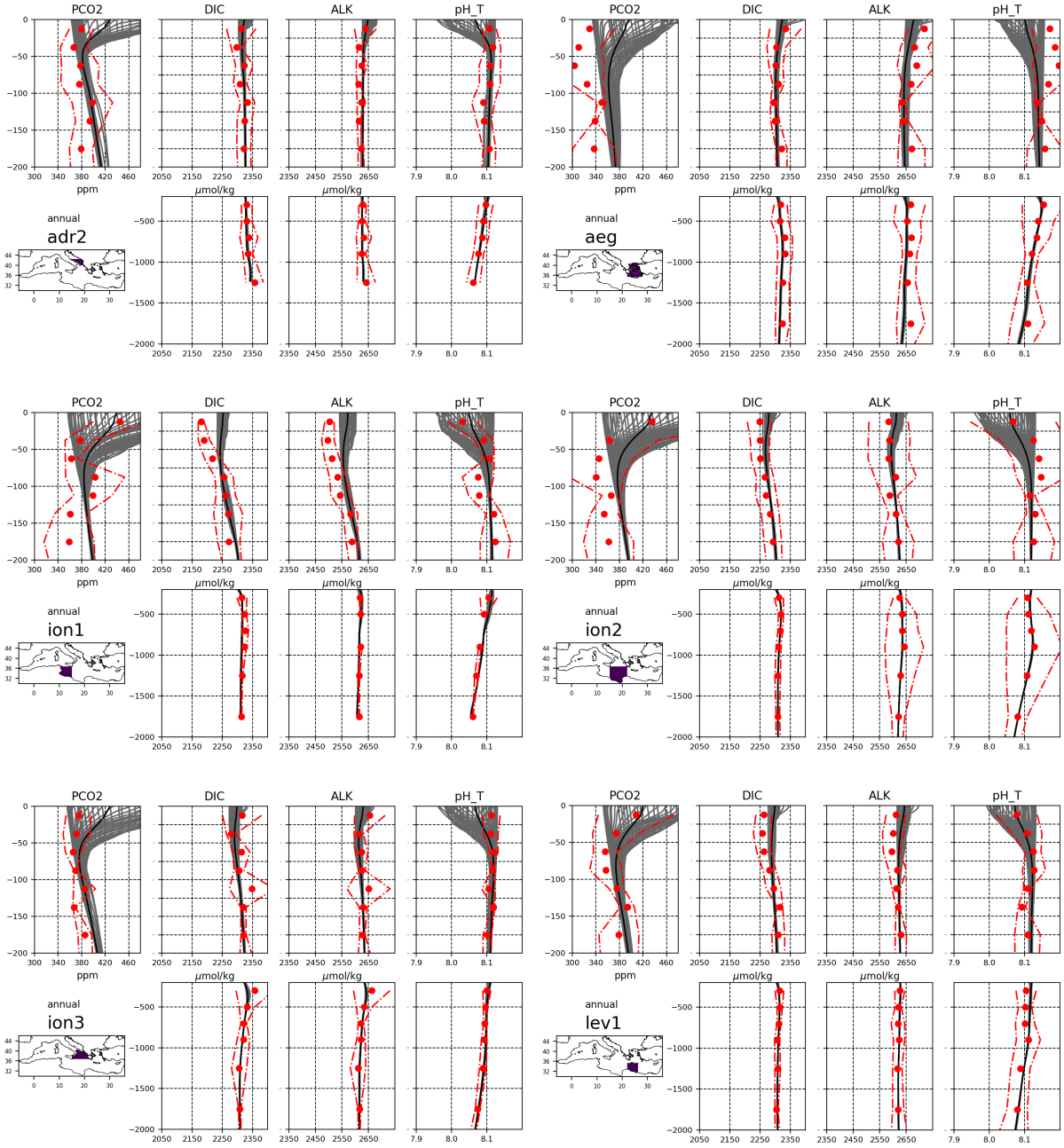

Figure IV.17. Continues overleaf.

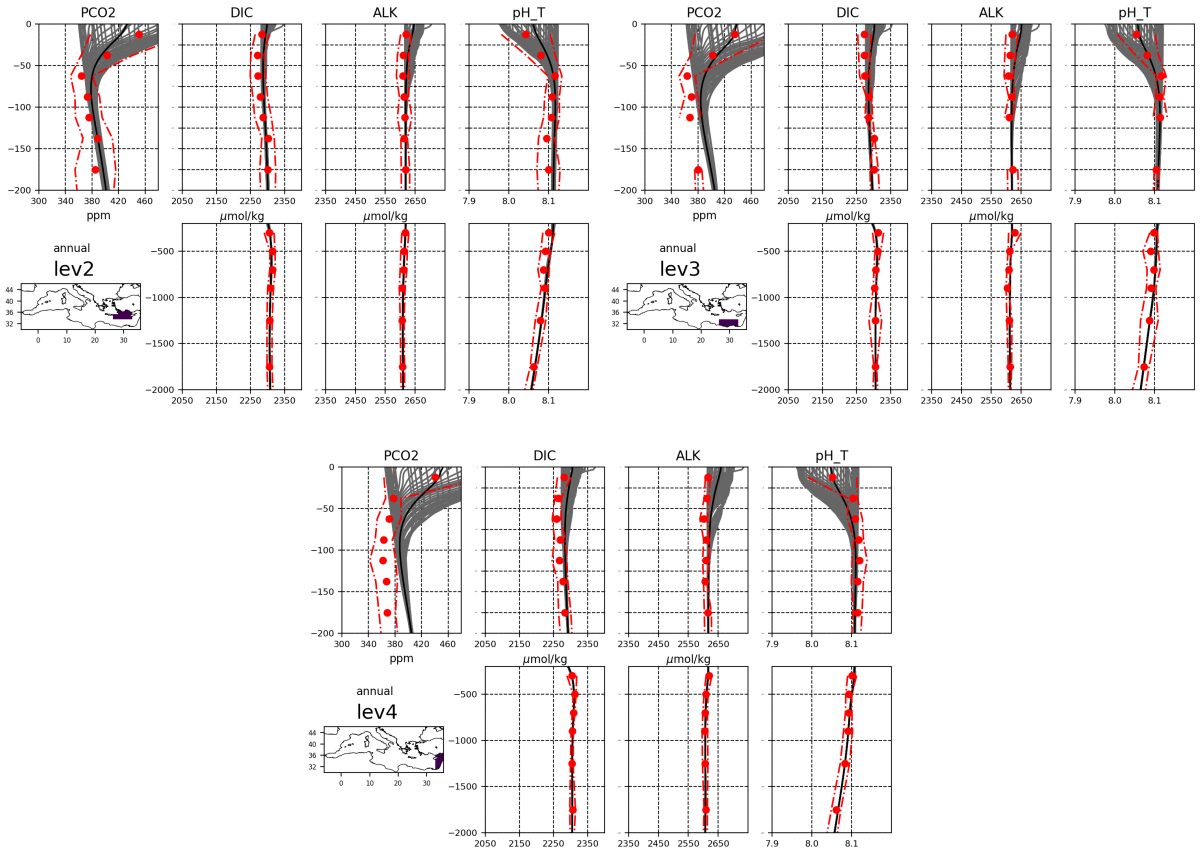

Figure IV.17. Profiles of pCO2, DIC, ALK and pH in total scale: mean weekly model profiles (grey color lines; from January to December 2017), mean annual model profiles (black lines) and CarbSys derived climatological (±standard deviation) profiles (red dots and dashed lines) for the sub-basins of Fig. III.1.

The model results and 1°x1° maps of climatology are reported in Figure IV.18 and 19 for ALK and DIC, respectively, showing a significant good agreement of the main basin-wide characteristics. In particular, a strong west-to-east surface gradient of both ALK and DIC is the main spatial pattern that can be recognized both on the model output and the climatology maps. The eastern marginal seas (Adriatic and Aegean Seas) are characterized by the highest values. The west-to-east gradient is a permanent structure recognizable at all depths, but less marked in the maps of the intermediate and deep layers (see for example the layer 150-300, right plots in Fig. IV.18 and 19). At the surface, DIC and ALK dynamics are driven by three major factors: the input in the eastern marginal seas (the terrestrial input from the Po and other Italian rivers and the input from the Dardanelles), the effect of evaporation in the eastern basin, and the influx of the low-ALK and low-DIC Atlantic waters in the western basin. The thermohaline basin-wide circulation modulates the intensity and the patterns of the spatial gradients. Intermediate and deep layers show weaker dynamics and less variability.

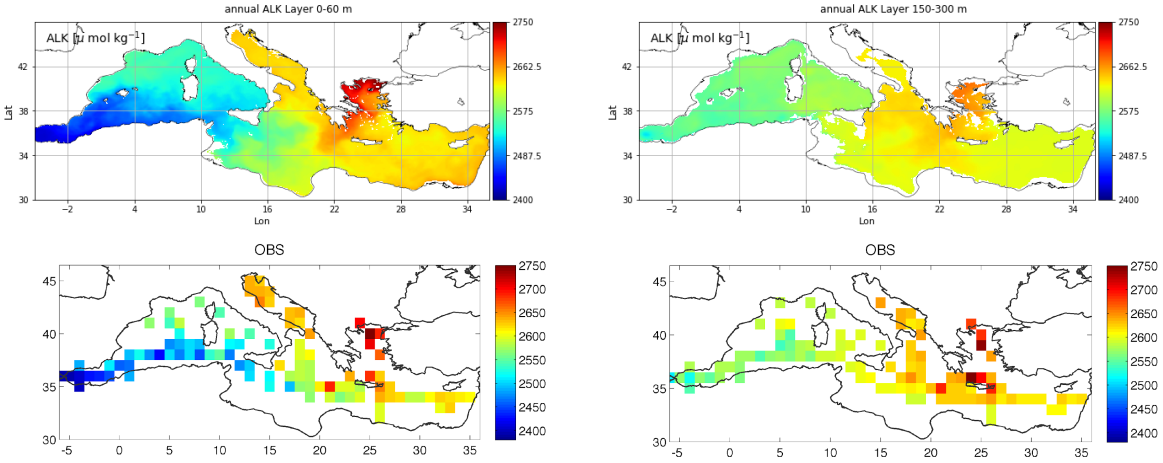

Figure IV.18. ALK mean annual maps of the 2017 qualification run (upper panels) and the 1°x1° climatology (lower panels) for the 0-60m (left) and 150-300 (right) layers.

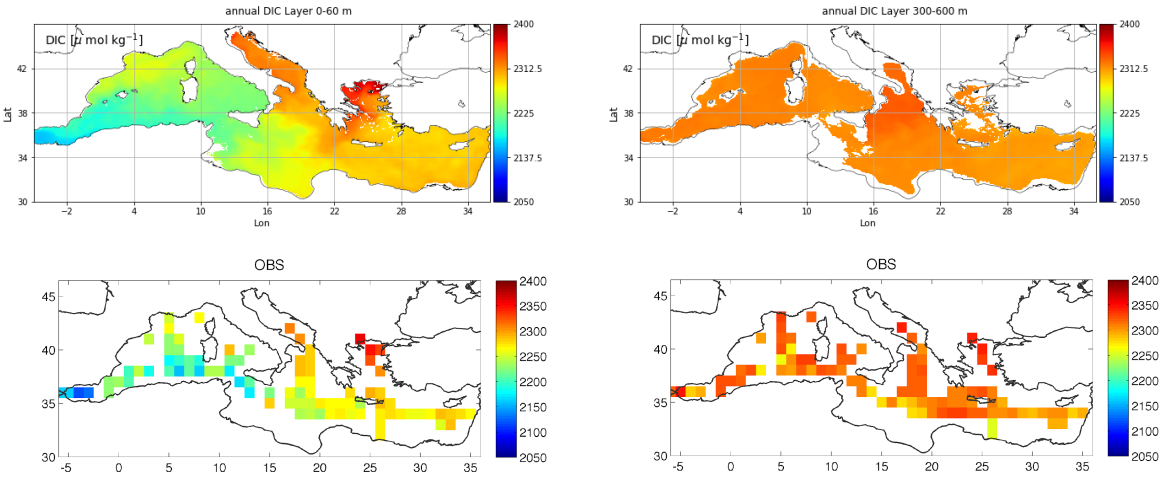

Figure IV.19. DIC mean annual maps of the 2017 qualification run (upper panels) and the 1°x1° climatology (lower panels) for the 0-60m (left) and 300-600 (right) layers.

At surface, the temperature effect on solubility mainly drives the modelled seasonal cycle of pCO2, while the spatial gradients of the carbonate system variables (DIC and ALK, Fig. IV.18 and 19) determines the heterogeneity of pCO2 among sub-basins. The MedBFM model reproduces fairly well both the seasonal cycle (i.e., maximum in summer and minimum in winter) and the main spatial differences between sub-basins as shown by the monthly climatology derived from the SOCAT dataset (Fig. IV.20). Indeed, nwm presents higher values than swm1 and alb, and ion1 has higher values than ion3. SOCAT dataset do not cover several sub-subasin (see Figure III.5). The overall uncertainty (i.e., RMSD of monthly values in sub-basins) of the surface pCO2, estimated using the novel SOCAT dataset, is of 49 µatm.

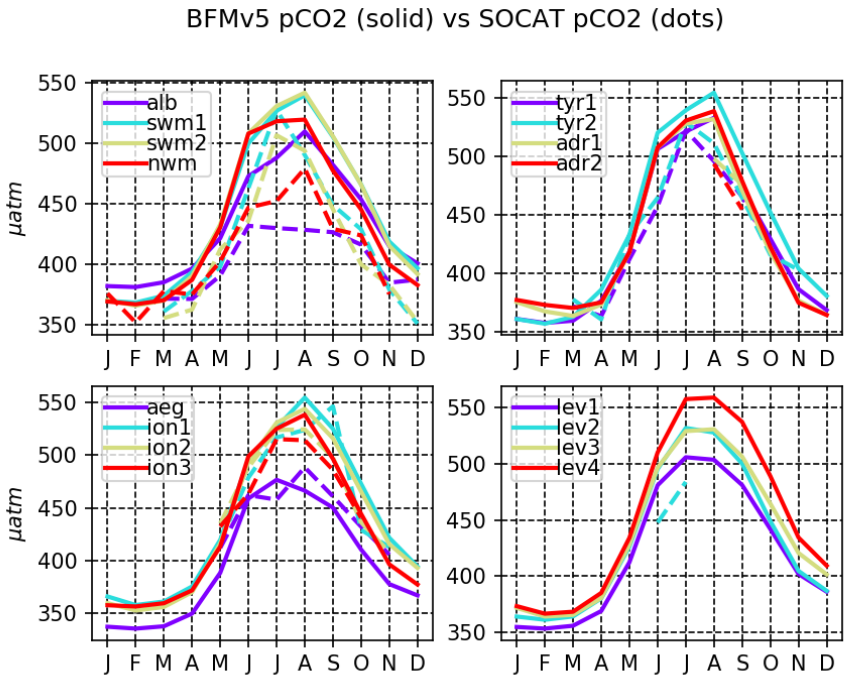

Figure IV.20. Monthly evolution of surface pCO2 [µatm] of model (solid lines) and climatology derived from SOCAT dataset (dashed lines when present) for the Mediterranean sub-basins.

III.6 CO2 air-sea flux

The modelled CO2 air-sea flux (Fig. IV.21) is compared with the MEDSEA_REANALYSIS_BIO_006_008 Reanalysis estimates published in the section 1.7 of the Ocean State Report (von Schuckmann et al., 2018) showing the consistency of the near real time product in reproducing the typical seasonal cycle of the air-sea fluxes with positive values (uptake of CO2 by the sea) during winter months and negative values (outgassing to the atmosphere) during summer months. The west to east gradient of the air-sea CO2 flux simulated by the operational product is fully consistent with the reanalysis product presented in the Ocean State Report.

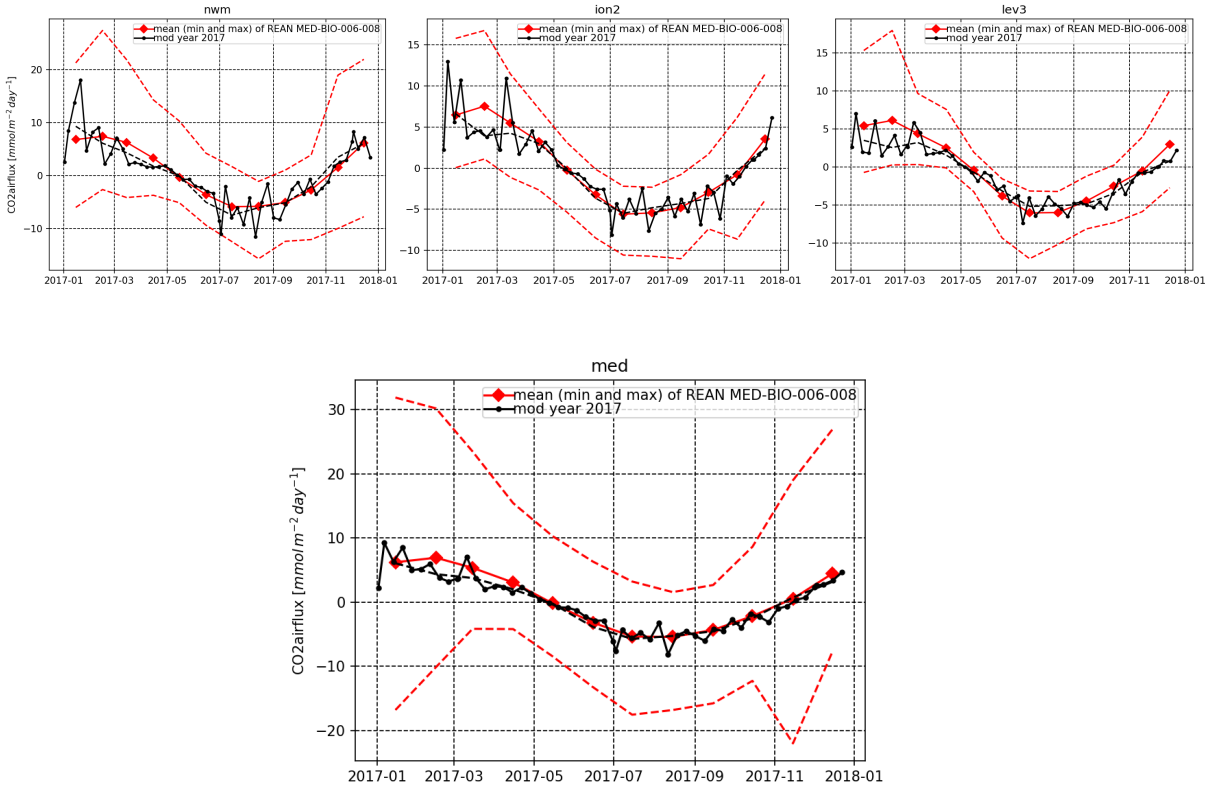

Figure IV.21. Air-sea CO2 fluxes [mmol m^{-2} d^{-1}] in the Mediterranean Sea and 3 selected sub-basins: simulation of year 2017 (back lines) and monthly climatology and its range derived from the Ocean State Report product (red lines).

IV SYSTEM'S NOTICEABLE EVENTS, OUTAGES OR CHANGES

Date	Change/Event description	System version	other
25/09/2017	First release of Mediterranean Sea biogeochemical analysis and forecast at 1/24° including assimilation of satellite chlorophyll over the entire domain	MedBFM2	V3.2 version
30/4/2018	Changes in the physical model (see CMEMS-MED-QUID-006-013 v1.1) and recalibration of boundary condition at the Atlantic buffer.	MedBFM2.1	V4.1 version
28/1/2018	Upgrade of the BFM model to the official version 5. Open boundary condition at the Dardanelles Strait consistently with the Med-PHY configuration.	MedBFM3.0	Q2/2019
6/12/2019	Upgrade of the 3DVarBio data assimilation scheme with assimilation of BGC-Argo floats data and daily forecast production cycle	MedBFM3.1	Q1/2020

V QUALITY CHANGES SINCE PREVIOUS VERSION

The present version differs from the previous one for the following points.

- The implementation of assimilation of vertical profiles of chlorophyll and nitrate from BGC-Argo floats has improved model performance in reproducing phytoplankton and nutrients dynamics in the area impacted by the float assimilation. However, it must be considered that the number of BGC-Argo floats greatly varies from year to year (e.g., 26 and 18 in 2018 and 2019 for chlorophyll), and that the BGC-Argo float coverage among sub-basins varies as well. (i.e., the BGC-Argo observing system program is not fully established yet). Thus, information assimilated and validation metrics can change substantially over time.
- The use of new reference for validation (i.e., the integration of the EMODnet dataset and the NODC-OGS dataset) allowed for the more accurate calculation of reference profiles among the sub-subsin and a more detailed assessment of the model performance.
- The daily production of 10-day forecast allows the MED-BIO products to be better aligned with the MED-PHY results.

VI REFERENCES

Álvarez, M.; Sanleón-Bartolomé, H.; Tanhua, T.; Mintrop, L.; Luchetta, A.; Cantoni, C.; Schroeder, K.; Civitarese, G. (2014) The CO2 system in the Mediterranean Sea: a basin wide perspective, Ocean Science, 10(1), pp.69-92

Bakker, D. C. E., Pfeil, B. Landa, C. S., Metzl, N., O'Brien, K. M., Olsen, A., Smith, K., Cosca, C., Harasawa, S., Jones, S. D., Nakaoka, S., Nojiri, Y., Schuster, U., Steinhoff, T., Sweeney, C., Takahashi, T., Tilbrook, B., Wada, C., Wanninkhof, R., Alin, S. R., Balestrini, C. F., Barbero, L., Bates, N. R., Bianchi, A. A., Bonou, F., Boutin, J., Bozec, Y., Burger, E. F., Cai, W.-J., Castle, R. D., Chen, L., Chierici, M., Currie, K., Evans, W., Featherstone, C., Feely, R. A., Fransson, A., Goyet, C., Greenwood, N., Gregor, L., Hankin, S., Hardman-Mountford, N. J., Harlay, J., Hauck, J., Hoppema, M., Humphreys, M. P., Hunt, C. W., Huss, B., Ibánhez, J. S. P., Johannessen, T., Keeling, R., Kitidis, V., Körtzinger, A., Kozyr, A., Krasakopoulou, E., Kuwata, A., Landschützer, 3 P., Lauvset, S. K., Lefèvre, N., Lo Monaco, C., Manke, A., Mathis, J. T., Merlivat, L., Millero, F. J., Monteiro, P. M. S., Munro, D. R., Murata, A., Newberger, T., Omar, A. M., Ono, T., Paterson, K., Pearce, D., Pierrot, D., Robbins, L. L., Saito, S., Salisbury, J., Schlitzer, R., Schneider, B., Schweitzer, R., Sieger, R., Skjelvan, I., Sullivan, K. F., Sutherland, S. C., Sutton, A. J., Tadokoro, K., Telszewski, M., Tuma, M., Van Heuven, S. M. A. C., Vandemark, D., Ward, B., Watson, A. J., Xu, S. (2016) A multi-decade record of high quality fCO2 data in version 3 of the Surface Ocean CO2 Atlas (SOCAT). Earth System Science Data 8: 383-413. doi:10.5194/essd8-383-2016.

Berner, R. A., & Morse, J. W.,1974. Dissolution kinetics of calcium carbonate in sea water; IV, Theory of calcite dissolution. American Journal of Science, 274(2), 108-134.

Bergametti, G., Remoudaki, E., Losno, R., Steiner, E., Chatenet, B., 1992. Source, transport and deposition of atmospheric Phosphorus over the northwestern Mediterranean, J. Atmos. Chem., 14, 501–513.

Bethoux, J. P., Morin, P., Chaumery, C., Connan, O., Gentili, B., and Ruiz-Pino, D., 1998. Nutrients in the Mediterranean Sea, mass balance and statistical analysis of concentrations with respect to environmental change, Mar. Chem., 63, 155–169.

Bosc, E., Bricaud, A., & Antoine, D. (2004). Seasonal and interannual variability in algal biomass and primary production in the Mediterranean Sea, as derived from 4 years of SeaWiFS observations. Global Biogeochemical Cycles, 18(1).

Copin-Montegut C., 1993. Alkalinity and carbon budgets in the Mediterranean Sea. Global Biogeochemical Cycles, 7(4), pp. 915-925.

Cornell, S., Rendell, A., Jickells, T., 1995. Atmospheric inputs of dissolved organic Nitrogen to the oceans, Nature, 376, 243–246.

Cossarini, G., Lazzari, P., Solidoro, C., 2015. Spatiotemporal variability of alkalinity in the Mediterranean Sea. Biogeosciences, 12(6), 1647-1658.

Crise, A., Solidoro, C., and Tomini, I.: Preparation of initial conditions for the coupled model OGCM and initial parameters setting, MFSTEP report WP11, subtask 11310, 2003.

de la Paz, M., Huertas, E.M., Padín, X.-A., Gónzalez-Dávila, M., Santana-Casiano, M., Forja, J.M., Orbi, A., Pérez, F.F., Ríos, A.F., Reconstruction of the seasonal cycle of air–sea CO2 fluxes in the Strait of Gibraltar, In Marine Chemistry, Volume 126, Issues 1–4, 2011, Pages 155-162.

Dobricic, S., Pinardi, N., 2008. An oceanographic three-dimensional variational data assimilation scheme. Ocean Modelling, 22, 3-4, 89-105.

Foujols, M.-A., Lévy, M., Aumont, O., Madec, G., 2000. OPA 8.1 Tracer Model Reference Manual. Institut Pierre Simon Laplace, pp. 39.

Guerzoni, S., Chester, R., Dulac, F., Herut, B., Loÿe-Pilot, M.-D., Measures, C., Migon, C., Molinaroli, E., Moulin, C., Rossini, P., Saydam, C., Soudine, A., Ziveri, P., 1999. The role of atmospheric deposition in the biogeochemistry of the Mediterranean Sea. Prog. Oceanogr., 44 (1-3): 147-190.

Herut, B. and Krom, M.: Atmospheric input of nutrients and dust to the SE Mediterranean, in: The Impact of Desert Dust Across the Mediterranean, edited by: Guerzoni, S. and Chester, R., Kluwer Acad., Norwell, Mass., 349–358, 1996.

Huertas, I. E., Ríos, A. F., García-Lafuente, J., Makaoui, A., Rodríguez-Gálvez, S., Sánchez-Román, A., Orbi, A., Ruíz, J., and Pérez, F. F.: Anthropogenic and natural CO2 exchange through the Strait of Gibraltar, Biogeosciences, 6, 647-662, 2009.

Kempe, S., Pettine M., Cauwet, G., 1991. Biogeochemistry of european rivers. In Degensempe & Richey eds, biogeochemistry of Major World Rivers, SCOPE 42 John Wiley 169-211

Kourafalou, V. H., & Barbopoulos, K. (2003). High resolution simulations on the North Aegean Sea seasonal circulation. In Annales Geophysicae (Vol. 21, No. 1, pp. 251-265).

Krasakopoulou E., Souvermezoglou E., Giannoudi L., Goyet C., 2017. Carbonate system parameters ad anthropogenic CO2 in the North Aegean Sea during October 2013. Continental Shelf Research, 149, 69-81.

Krom, M.D., Kress, N., Brenner, S., Gordon, L.I., 1991. Phosphorus limitation of primary productivity in the eastern Mediterranean Sea. Limnology and Oceanography, 36(3) 424-432.

Lazzari, P., Teruzzi, A., Salon, S., Campagna, S., Calonaci, C., Colella, S., Tonani, M., Crise, A. 2010. Pre-operational short-term forecasts for the Mediterranean Sea biogeochemistry. Ocean Science, 6, 25-39.

Lazzari, P., Solidoro, C., Ibello, V., Salon, S., Teruzzi, A., Béranger, K., Colella, S., and Crise, A., 2012. Seasonal and inter-annual variability of plankton chlorophyll and primary production in the Mediterranean Sea: a modelling approach. Biogeosciences, 9, 217-233.

Lazzari, P., Solidoro, C., Salon, S., Bolzon, G., 2016. Spatial variability of phosphate and nitrate in the Mediterranean Sea: a modelling approach. Deep Sea Research I, 108, 39-52.

Lueker, T. J., Dickson, A. G., and Keeling, C. D.: Ocean pCO2 calculated from dissolved inorganic carbon, alkalinity, and equations for K1 and K2: validation based on laboratory measurements of CO2 in gas and seawater at equilibrium, Mar. Chem., 70, 105–119, 2000.

Mehrbach, C., Culberson, C. H., Hawley, J. E., and Pytkowitcz, R. M.: Measurements of the apparent dissociation constants of carbonic acid in seawater at atmospheric pressure, Limnol. Oceanogr., 18, 897–907, 1973.

Meybeck M., Ragu A., 1995 River Discarges to the Oceans: An Assessment of suspended solids, major ions and nutrients UNEP STUDY

Mignot A., F. D'Ortenzio, V. Taillandier, G. Cossarini, S. Salon, L. Mariotti, 2017. Estimation of BGC-Argo chlorophyll fluorescence and nitrate observational errors using the triple collocation method. 6th Euro-Argo Users Meeting July 4-5, 2017 in Paris, France.

Loÿe-Pilot, M. D., J. M. Martin, and J. Morelli, 1990. Atmospheric input of inorganic nitrogen to the western Mediterranean. Biogeochem., 9: 117-134.

Deliverable D4.6: SES land-based runoff and nutrient load data (1980 -2000), edited by Bouwman L. and van Apeldoorn D., 2012 PERSEUS H2020 grant agreement n. 287600.

Orr and Epitaloni, 2015: "Improved routines to model the ocean carbonate system: mocsy 2.0." GMD 8.3 : 485-499.

Orr, J. C., Najjar, R. G., Aumont, O., Bopp, L., Bullister, J. L., Danabasoglu, G., ... & Griffies, S. M., 2017. Biogeochemical protocols and diagnostics for the CMIP6 Ocean Model Intercomparison Project (OMIP), Geosci. Model Dev., 10, 2169–2199.Petihakis, G., Tsiara, K., Triantafyllou, G., Kalaroni, S., & Pollani, A. (2014). Sensitivity of the N. AEGEAN SEA ecosystem to Black Sea Water inputs. Mediterranean Marine Science, 15(4), 790-804. doi:http://dx.doi.org/10.12681/mms.955

Ribera d'Alcalà M., Civitarese G., Conversano F., Lavezza R., 2003. Nutrient ratios and fluxes hint at overlooked processes in the Mediterranean Sea. Journal of Geophysical Research, 108(C9), 8106, doi:10.1029/2002JC001650.

Salon, S., Cossarini, G., Bolzon, G., Feudale, L., Lazzari, P., Teruzzi, A., Solidoro, C., Crise, A., 2019. Marine Ecosystem forecasts: skill performance of the CMEMS Mediterranean Sea model system. Ocean Sci. Discuss. 1–35. https://doi.org/10.5194/os-2018-145

Schneider, A., Wallace, D. W. R., and Kortzinger, A.: Alkalinity of the Mediterranean Sea, Geophys. Res. Lett., 34, L15608, doi:10.1029/2006GL028842, 2007.

Somot, S., Sevault, F., Déqué, M., Crépon, M., 2008. 21st century climate change scenario for the Mediterranean using a coupled atmosphere–ocean regional climate model, Global and Planetary Change, 63, 2–3: 112–126.

Souvermezoglou, E., Krasakopoulou, E., Pavlidou, A., 2014. Temporal and spatial variability of nutrients and oxygen in the North Aegean Sea during the last thirty years. Mediterranean Marine Science, 15/4, 805-822.

Teruzzi, A., Dobricic, S., Solidoro, C., Cossarini, G. 2014. A 3D variational assimilation scheme in coupled transport biogeochemical models: Forecast of Mediterranean biogeochemical properties, Journal of Geophysical Research, doi:10.1002/2013JC009277.

Teruzzi, A., Bolzon, G., Salon, S., Lazzari, P., Solidoro, C., Cossarini, G., 2018. Assimilation of coastal and open sea biogeochemical data to improve phytoplankton simulation in the Mediterranean Sea. Ocean Modelling, 132, 46-60

Teruzzi, A., Di Cerbo, P., Cossarini, G., Pascolo, E., Salon, S., 2019. Parallel implementation of a data assimilation scheme for operational oceanography: the case of the MedBFM model system, submitted to Computers & GeosciencesTeruzzi, A., Bolzon, G., Salon, S., Lazzari, P., Solidoro, C., and Cossarini, G. (2018). Assimilation of coastal and open sea biogeochemical data to improve phytoplankton simulation in the mediterranean sea. Ocean Modelling, 132:46–60.

Thingstad, T.F., Rassoulzadegan, F., 1995. Nutrient limitations, microbial food webs, and 'biological C-pumps': suggested interactions in a P-limited Mediterranean. Marine Ecology Progress Series, 117: 299-306.

Tugrul, S., Besiktep,e T., Salihoglu, I., 2002. Nutrient exchange fluxes between the Aegean ad tBlack Seas through the Marmara Sea. Mediterranean Marine Science, 3/1, 33-42.

von Schuckmann, K., Le Traon, P.Y., Smith, N., Pascual, A., Brasseur, P., Fennel, K. and Djavidnia, S., et al., 2018. Copernicus marine service ocean state report. Journal of Operational Oceanography, 11(sup1), pp.S1-S142.

World Ocean Atlas 2013 database, https://www.nodc.noaa.gov/OC5/woa13/

Yalcin B., Artuz M.L., Pavlidou A., Cubuk S., Dassenakis M., 2017. Nutrient dynamics and eutrophication in the Sea of Marmara: data from recent oceanographic research. Science of the Total Environment, 601-602, 405-424.

Zeebe, R.E. and Wolf Gladrow, D., 2001. CO2 in seawater: equilibrium, kinetics, isotopes, Elsevier oceanography series. Elsevier.

Wanninkhof 2014, OCMIP2 design document & OCMIP2 Abiotic HOWTO. Limnol. Oceanograph. Methods, 12, 351-362.